

Redshift in a six-dimensional classical Kaluza-Klein type model

Jacek Syska

Department of Field Theory and Particle Physics, Institute of Physics, University of Silesia, Uniwersytecka 4, 40-007 Katowice, Poland

E-mail: jacek.syska@us.edu.pl

Abstract. Multidimensional theories still remain attractive from the point of view of better understanding fundamental interactions. In this paper a six-dimensional Kaluza-Klein type model at the classical, Einstein's gravity formulation is considered. The static spherically symmetric solution of the six-dimensional Einstein equations coupled to the Klein-Gordon equation with the massless dilatonic field is presented. As it is horizon free, it is fundamentally different from the four-dimensional Schwarzschild solution. The motion of test particles in such a spherically symmetric configuration is then analyzed. The presence of the dilatonic field has a similar dynamical effect as the existence of additional massive matter. The emphasis is put on some observable quantities like redshifts. It has been suggested that strange features of emission lines from galactic nuclei as well as quasar-galaxy associations may in fact be manifestations of the multidimensionality of the world.

Keywords: multidimensional theories, Hamilton-Jacobi equation, redshifts, quasar-galaxy associations

1. Introduction

And do not be called teachers;
for One is your Teacher,
the Christ *Jesus*.

Holy Bible, Matthew 23:10

Let the gravitational interaction be described by the Einstein equations [1], [2], [3] and let us suppose that space-time is more than four dimensional [4]. In fact, many 20th century ideas of theoretical physics introduced the possibility that the world may be multidimensional [5]. Among them are the Kaluza-Klein theories [6] and despite some problems the continued interest in them also stems from the fact that the isometry group of the metric on the extra-dimensional compact internal space generates gauge symmetries of the resulting four-dimensional (non-Abelian) gauge theories [7, 8]. In order that a multidimensional theory, e.g. a ten-dimensional superstring one, could be taken as the physically accepted one, it should possess the proper four-dimensional phenomenology, primarily the observed bosonic and fermionic fields spectrum [9]. In this context, new results from the large hadron collider (LHC) experiment are still awaited, including the adjustment of all experimental results [10].

Yet, even if the extra-dimensions effect were noticed in the LHC experiment, the interpretation of this fact could possibly possess the side affect of the (recently increasing) problems, which lie behind the experimental validation of the uncertainty relation (UR) [11]. In that context, two effects can compete and both of them necessitate a deep theoretical reformulation of UR [12]. The first effect is connected with e.g. i) the diffraction-interferometric experiments for a photon, where both the uncertainty relation and the meaning of the half-widths of a pair of functions (time and frequency) related by the Fourier transform is examined [13, 14] and ii) an experiment of the successive projective measurements of two non-commuting neutron spin components [15]. In these experiments gravitational effects are not perceived and the decrease of the right-hand side of the UR, where the Plank constant is, is possibly observed. The second effect is connected with the space-time curvature impact, which makes the value of the uncertainty of the distance in the coordinate basis bigger than the true one (compare Eq.(37)). These mean that the Plank constant is in practice multiplied by a constant or functional factor [11, 16] and in the observation becomes the effective one [17]. To sum up, the problems [18], [19] with the UR and effectiveness of the Plank constant could be mistakenly taken as the signal from the extra dimensions in the accelerator experiments.

Meanwhile, there were also attempts in the literature to seek the effects of the internal space with a small number of extra dimensions (one or two) in an astrophysical setting. Previously, these were pursued by Wesson, Lim, Kalligas, Everitt [20] for one extra dimension and Biesiada, Mańka, Syska [21, 22, 23] for two extra dimensions. This line

of thinking is worth developing in order to gain a better understanding of the possible visibility of manifestations of e.g. the six-dimensionality of the world, not only in the astrophysical observations but, also in particle experiments [24]. This would mean that the effects of extra dimensions may well be around us [25] in contrast to standard expectations that extremely high energies are indispensable to probe higher dimensions in search of their existence [26].

The contents of the present paper suggest that there is an intimate relation between the manifestations of the six-dimensionality of this world and so-called dark matter (not dark energy). The first conjecture on the existence of dark matter in galaxies came into play when Oort [27] in 1932 and Zwicky [28] in 1933 applied the famous virial theorem to the vertical motion of the stars in the Milky Way and to the radial velocities of members of the Coma cluster, respectively, or even earlier in 1915 when Öpik [29] evaluated the dynamical density of matter in the Milky Way in the vicinity of the sun. The problem was revived and became well established in the seventies when it was demonstrated [30, 31] that the rotation curves of spiral galaxies were indicative of the possible presence of a zero luminosity, dark mass, i.e. unseen in any part of electromagnetic spectrum (except for the visibility of possible matter which would be its own antimatter). There have been many suggestions for candidates for dark matter, from the possibly insufficient impact of massive compact halo objects (MACHOs) [32] such as “brown dwarfs”, “standard” neutron stars, “nomad planets” etc. at the one extreme to hypothetical elementary particles like massive neutrinos, axions and other weakly interacting massive particles (WIMPs), which till now are either unable to give the amount of mass needed or are in contradiction with other parts of proposed models [33]. What precisely is dark matter in any detection? Thus, one of the questions is: What, from the scientific point of view, are the inflationary models of all sorts with the persistent lack of observations of their main building blocks, i.e. dark matter and dark energy?

The present paper provides a description of the properties of a certain six-dimensional Kaluza-Klein type model. Section 2 contains a description of the model along with motivations for the choice of six-dimensional space-time (see also [24]). Then, the static spherically symmetric solutions of the multidimensional Einstein equations coupled to the Klein-Gordon equation with the massless dilatonic field [34] are derived [23, 35, 22]. They are in a sense analogous to the familiar four-dimensional Schwarzschild solution but fundamentally different i.e. they are horizon free. A more detailed discussion of the properties of these solutions is presented in Sections 2 and 3. Some strictly observable quantities, such as the redshift formulae, are also briefly discussed. Section 4 is devoted to the analysis of the motion of test particles ruled by the six-dimensional Hamilton-Jacobi equation. The application of the obtained background self-consistent solution [23] in the description of the wave-mechanical structure of e.g. the neutron and its excited states can be found in [24]. Some possible astrophysical and cosmological observational consequences of the model are also presented in Section 4 and in Section 6, which also contains concluding remarks and perspectives. They refer

exclusively to relatively tight systems, e.g. the vicinity of a galactic nucleus and a binary galaxy or galaxy-quasar system. The scale invariance of the model is discussed in Section 5. Several more formal, although important, remarks are in the Appendices at the end of this paper. Throughout Section 2 the natural units ($c = \hbar = 1$) are used whereas in Sections 3, 4 and 6, which deal with some more observationally oriented issues, the velocity of light is reintroduced explicitly (the Planck constant is irrelevant for this paper considerations).

2. Field equations

The simplest extension of the familiar four-dimensional space-time models are five-dimensional ones, which were previously considered by Wesson [20]. In the present paper a six - dimensional model that is more robust is presented. The motivations for choosing six-dimensional models by many others were quite diverse. For example, as late as the years 1984-1986, Nishino, Sezgin, Salam and Bergshoeff in [36] suggested that one can obtain the fermion spectrum by the compactification of the extra two dimensions in a supersymmetric model. Also, the six-dimensional models of the Kaluza-Klein theory were previously investigated by Ivashchuk and Melnikov [37], Bronnikov and Melnikov [38] and by Mańka and Syska [21].

In [24] the statistical, Fisher informational reason for the six-dimensionality of space-time was given and the geometrical properties of the resulting six-dimensional Kaluza-Klein type model [39], from the point of view of its impact on the structure of the neutron and its excited states, were also investigated. The common point of that model [24] and the one presented below is the basic massless scalar (dilaton) field obtained simultaneously with the metric tensor field as the self-consistent solution of the coupled Einstein and Klein-Gordon equations. Then, the obtained metric serves as the background for the equation of motion of the new *added object*, which can be a field [24] or a classical test particle, immersed in the background metric. The idea of covering the physical structures that are extremely remote in size by one type of mathematical solution is known by the term of scaling in both theoretical and experimental physics [40]. In this respect, both models, the current one and the one presented in [24] possess the same Kaluza-Klein type self-consistent background solution, which formally can be scaled to all distances. More on this can be found in [24] (see also Section 5). Yet, whereas in [24] the *added object* is governed by the Klein-Gordon equation solved (not self-consistently) in the mentioned background metric and the solution is a wave-mechanical one, in the present paper the added object is the classical test particle moving in accordance with the Hamilton-Jacobi equation.

Thus, let us consider a six-dimensional field theory model comprising the gravitational self field described by a metric tensor, g_{MN} , and a real massless “basic” scalar field, φ . This scalar field φ is a dilatonic field hence, just below, the minus sign is present in front of its kinetic energy term [23, 35]. In a standard manner we decompose the action

into two parts

$$\mathcal{S} = \mathcal{S}_{EH} + \mathcal{S}_\varphi , \quad (1)$$

where \mathcal{S}_{EH} is the Einstein–Hilbert action

$$\mathcal{S}_{EH} = \int d^6x \frac{1}{2\kappa_6} \sqrt{-g} \mathcal{R} \quad (2)$$

and \mathcal{S}_φ is the action for a real massless dilatonic field

$$\mathcal{S}_\varphi = \int d^6x \sqrt{-g} \mathcal{L}_\varphi = - \int d^6x \sqrt{-g} \frac{1}{2} g_{MN} \partial^M \varphi \partial^N \varphi . \quad (3)$$

In Eqs.(2),(3), $g = \det g_{MN}$ denotes the determinant of the metric tensor, \mathcal{R} is the curvature scalar of six-dimensional (in general curved) space-time and κ_6 denotes the coupling constant of the six-dimensional theory, which is analogous to the familiar Newtonian gravity constant. \mathcal{L}_φ is the Lagrangian density for a dilatonic massless field φ .

By extremalizing the action given by Eqs.(1)-(3), we obtain the Einstein equations

$$G_{MN} = \kappa_6 T_{MN} , \quad (4)$$

where $G_{MN} = R_{MN} - \frac{1}{2} g_{MN} \mathcal{R}$ is the Einstein tensor, R_{MN} is the six-dimensional Ricci tensor and T_{MN} is the energy-momentum tensor of a real dilatonic field φ , which is given by

$$T_N^M = \partial_N \varphi \frac{\partial \mathcal{L}_\varphi}{\partial (\partial_M \varphi)} - \delta_N^M \mathcal{L}_\varphi . \quad (5)$$

Variation of the total action \mathcal{S} with respect to the field φ gives the Klein-Gordon equation

$$\square \varphi = 0 , \quad (6)$$

where

$$\square = - \frac{1}{\sqrt{-g}} \partial_M (\sqrt{-g} g^{MN} \partial_N) \quad (7)$$

and g^{MN} is the tensor dual to g_{MN} .

Now, we assume that we live in the compactified (which is quite a reasonable assumption) world, where the six-dimensional space-time is a topological product of “our” curved four-dimensional physical space-time (with the metric $g_{\alpha\omega}$, $\alpha, \omega = 0, 1, 2, 3$) and the internal space (with the metric g_{he} , $h, e = 5, 6$). Therefore, the metric tensor can be factorized as follows

$$g_{MN} = \begin{pmatrix} g_{\alpha\omega} & 0 \\ 0 & g_{he} \end{pmatrix} . \quad (8)$$

The four-dimensional diagonal part is assumed to be that of a spherically symmetric geometry

$$g_{\alpha\omega} = \begin{pmatrix} e^{\nu(r)} & & & \\ & -e^{\mu(r)} & 0 & \\ & 0 & -r^2 & \\ & & & -r^2 \sin^2 \Theta \end{pmatrix} , \quad (9)$$

where $\nu(r)$ and $\mu(r)$ are (at this stage) two arbitrary functions. Analogously, we take the two-dimensional internal part to be

$$g_{he} = \begin{pmatrix} -\varrho^2(r) \cos^2\vartheta & 0 \\ 0 & -\varrho^2(r) \end{pmatrix}. \quad (10)$$

The six-dimensional coordinates (x^M) are denoted by $(t, r, \Theta, \Phi, \vartheta, \varsigma)$, where $t \in [0, \infty)$ is the usual time coordinate, $r \in [0, \infty)$, $\Theta \in [0, \pi]$ and $\Phi \in [0, 2\pi)$ are familiar three-dimensional spherical coordinates in the macroscopic space; $\vartheta \in [-\pi, \pi)$ and $\varsigma \in [0, 2\pi)$ are coordinates in the internal two-dimensional parametric space and $\varrho \in (0, \infty)$ is the “radius” of this two-dimensional internal space. We assume that $\varrho(r)$ is the function of the radius r in our external three-dimensional space [41].

The internal space is a 2-dimensional parametric space with an r -dependent parameter $\varrho(r)$, which can be represented as a surface embedded in the three-dimensional Euclidean space

$$\begin{cases} w^1 = \varrho(r) \cos\varsigma & , \quad \varsigma \in [0, 2\pi) \\ w^2 = \varrho(r) \sin\varsigma \\ w^3 = \varrho(r) \sin\vartheta & , \quad \vartheta \in [-\pi, \pi) . \end{cases} \quad (11)$$

Now using Eqs.(9)-(10), we can calculate the components of the Ricci tensor. The nonvanishing components are [23]

$$R_t^t = (4 \varrho^2 r \nu' + 4 r^2 \varrho' \varrho \nu' - r^2 \varrho^2 \mu' \nu' + r^2 \varrho^2 (\nu')^2 + 2 r^2 \varrho^2 \nu'') (4 e^\mu r^2 \varrho^2)^{-1} \quad (12)$$

$$R_r^r = (-4 \varrho^2 r \mu' - 4 r^2 \varrho' \varrho \mu' - r^2 \varrho^2 \mu' \nu' + r^2 \varrho^2 (\nu')^2 + 8 r^2 \varrho \varrho'' + 2 r^2 \varrho^2 \nu'') (4 e^\mu r^2 \varrho^2)^{-1} \quad (13)$$

$$R_\Theta^\Theta = R_\Phi^\Phi = (-4 e^\mu \varrho^2 + 4 \varrho^2 + 8 r \varrho \varrho' - 2 r \varrho^2 \mu' + 2 r \varrho^2 \nu') (4 e^\mu r^2 \varrho^2)^{-1} \quad (14)$$

$$R_\vartheta^\vartheta = R_\varsigma^\varsigma = (8 \varrho r \varrho' + 4 r^2 (\varrho')^2 - 2 r^2 \varrho \varrho' \mu' + 2 r^2 \varrho \varrho' \nu' + 4 r^2 \varrho \varrho'') (4 e^\mu r^2 \varrho^2)^{-1}. \quad (15)$$

Let us assume that we are looking for a solution of the Einstein equations (see Eq.(4)) with the Ricci tensor given by Eqs.(12)-(15), with $\nu(r) = \mu(r)$, and with the following boundary conditions

$$\lim_{r \rightarrow \infty} \nu(r) = \lim_{r \rightarrow \infty} \mu(r) = 0, \quad (16)$$

$$\lim_{r \rightarrow \infty} \varrho(r) = d = \text{constant} \neq 0. \quad (17)$$

In other words, we are looking for the solution which at spatial infinity reproduces the flat external four-dimensional Minkowski space-time and static internal parametric space of “radius” d , which could be of the order of $10^{-33} m$. However, a much higher value of d for the discussed background field configuration, which has, from the point

of view of particle physics a very interesting phenomenology, is also possible (compare [24], where for the neutron $d \sim 10^{-16} m$).

Now, we make an assumption that the dilatonic field φ depends neither on time t nor on the internal coordinates ϑ and ς . Because of assumed spherical symmetry of the physical space-time, it is natural to suppose that the dilatonic field φ is the function of the radius r alone

$$\varphi(x^M) = \varphi(r) . \quad (18)$$

We also impose a boundary condition for the dilatonic field φ

$$\lim_{r \rightarrow \infty} \varphi(r) = 0 , \quad (19)$$

which supplements boundary conditions (16) and (17) for the metric components.

By virtue of Eqs.(5) and (3), it is easy to see that the only nonvanishing components of the energy-momentum tensor are

$$-T_r^r = T_t^t = T_\Theta^\Theta = T_\Phi^\Phi = T_\vartheta^\vartheta = T_\varsigma^\varsigma = \frac{1}{2} g^{rr} (\partial_r \varphi)^2 . \quad (20)$$

Consequently, it is easy to verify that the solution of the Einstein equations (4) is

$$\nu(r) = \mu(r) = \ln \left(\frac{r}{r+A} \right) \quad (21)$$

$$\varrho(r) = d \sqrt{\frac{r+A}{r}} \quad (22)$$

$$\varphi(r) = \pm \sqrt{\frac{1}{2\kappa_6}} \ln \left(\frac{r}{r+A} \right) . \quad (23)$$

Hence, we obtain that the only nonzero component of the Ricci tensor (see Eqs.(12)-(15)) is R_r^r , which reads

$$R_r^r = \frac{A^2}{2 r^3 (r+A)} . \quad (24)$$

So the curvature scalar \mathcal{R} is equal to

$$\mathcal{R} = R_r^r = \frac{A^2}{2 r^3 (r+A)} , \quad (25)$$

where A is the real constant with the dimensionality of length, whose value is to be taken from observations for each particular system. In the derivation of the above solutions, we have used Eqs.(12)-(15), which together with Eq.(20) imply that all of the six diagonal Einstein equations are equal to just one

$$\frac{1}{2} \mathcal{R} = \kappa_6 T_r^r . \quad (26)$$

Remark: Putting Eqs.(26),(20) and (25) together we can notice a similarity between the equation

$$R_r^r = -\kappa_6 (\partial_r \varphi)^2 g^{rr} \quad (27)$$

and its electromagnetic analog $\nabla^2 \mathbf{A} = m_A^2 \mathbf{A}$, where \mathbf{A} is the electromagnetic vector potential. Eq.(27) is the (anti)screening current condition in gravitation that is analogous to that in electromagnetism or in the electroweak sector in the self-consistent approach [22, 42, 43].

Now, we can rewrite the metric tensor in the form

$$\begin{aligned} g_{MN} &= \text{diag} (g_{tt}, g_{rr}, g_{\Theta\Theta}, g_{\Phi\Phi}, g_{\vartheta\vartheta}, g_{\zeta\zeta}) = \\ &= \text{diag} \left(\frac{r}{r+A}, -\frac{r}{r+A}, -r^2, -r^2 \sin^2 \Theta, -d^2 \frac{r+A}{r} \cos^2 \vartheta, -d^2 \frac{r+A}{r} \right) \end{aligned} \quad (28)$$

with its determinant equal to

$$g = \det g_{MN} = -(d^2 r^2 \sin \Theta \cos \vartheta)^2 \quad (29)$$

that itself is nonsingular. We see that the space-time of the model is stationary.

It is also necessary to verify whether the solution of the Klein-Gordon equation (6) is in agreement with Eq.(23), which follows from the Einstein equations. According to Eq.(6) and Eqs.(18),(28),(29), we obtain that

$$\partial_r \varphi(r) = -C g_{rr} r^{-2} = C \frac{1}{r(r+A)}, \quad (30)$$

where C is a constant. Comparing this result with Eq.(23), we conclude that if

$$C = \pm \frac{A}{\sqrt{2\kappa_6}} \quad (31)$$

then the solution of the Klein-Gordon equation is in agreement with the solution of the Einstein equations coupled to the Klein-Gordon one. Hence, the real massless “basic” dilatonic field $\varphi(r)$ given by Eq.(23) can be the source of the nonzero metric tensor given by Eq.(28). Only when the constant A is equal to zero do the solutions (21)-(23) become trivial and the six-dimensional space-time is Ricci flat.

It is worth noting that because the components $R_{\vartheta}^{\vartheta}$ and R_{ζ}^{ζ} of the Ricci tensor are equal to zero for all values of A , the internal space is always Ricci flat. However, we must not neglect the internal parametric space because its “radius” ϱ is a function of r and the two spaces, external and internal, are therefore “coupled”. Only when $A = 0$ are these two spaces “decoupled” and our four-dimensional space-time becomes Minkowski flat.

Remark: When A is not equal to zero, our four-dimensional external space-time is curved. Its scalar curvature \mathcal{R}_4 is equal to (25)

$$\mathcal{R}_4 = \mathcal{R} = \frac{A^2}{2 r^3 (r+A)}. \quad (32)$$

2.1. The stability of the background solution

Let us consider the stability of the self-consistent gravito-dilatonic configuration given by Eqs. (23) and (28). We calculate its energy $E_{g+\varphi}$ (see [24]), which is the integral

over the spacelike hypersurface [8]

$$E_{g+\varphi} = \int_V d^5x \sqrt{-g} (G^{tt} + \kappa_6 T^{tt}) , \quad (33)$$

where using Eqs.(20)-(29) we obtain

$$E_{g+\varphi} = -2 \int_V d^5x \sqrt{-g} g^{tt} \frac{\mathcal{R}}{2} = -2 Q \leq 0 \quad (34)$$

and

$$Q = 8 d^2 \pi^2 \lim_{\varepsilon \rightarrow 0^+} \int_{\varepsilon}^{\infty} \frac{A^2}{r^2} dr = (2\pi d) (4\pi A^2) \lim_{\varepsilon \rightarrow 0^+} \frac{d}{\varepsilon} . \quad (35)$$

By using the Fisher information formalism, which was developed for the physical models by Frieden and others [44, 45, 19, 24, 46], the foundation of the partition of $E_{g+\varphi}$ in Eq.(33) into two parts, was constructed. The first term, G^{tt} , is connected with the Fisherian kinematical degrees of freedom of the gravitational configuration and the second one, T^{tt} , is connected with its structural degrees of freedom.

The integrand in Eq.(35) does not converge on $(0, \infty)$ for $A \neq 0$. If in Eq.(35), the cutoff $\varepsilon = d$ is taken [24], which breaks the self-consistency of the solution, then it leads to $Q = Q_{cut} = (2\pi d) (4\pi A^2)$ making Q_{cut} finite. The value of Q_{cut} could be small in contradistinction to the infinite value obtained in Eq.(35) for $\varepsilon \rightarrow 0$ taken in the self-consistent case. Hence, for $A \neq 0$, the self-consistent solution given by Eqs.(23) and (28), which has energy $E_{g+\varphi}$ given by Eq.(34), cannot be destabilized to yield any other with finite energy. The energy is the generic property of the solution [47]. In particular, if $\psi(B)$ is a well-behaved field [48] that depends on a parameter B , then it cannot be destabilized to any solution with the energy $E_{g+\psi(B)}$ from the sequence that has the limit $E_{g+\psi} \xrightarrow{B \rightarrow 0} 0$, which itself corresponds to $A = 0$. Hence, the transition from the self-consistent gravito-dilatonic configuration given by Eqs.(23) and (28) to any others with finite energy is forbidden [24].

Let us notice that the solution for $A = 0$ is consistent with the Minkowskian space-time one, which has global energy equal to zero [8]. Therefore, the condition on the right hand side of Eq.(34) indicates that the self-consistent gravito-dilatonic configuration given by Eqs. (23) and (28) for $A \neq 0$ is more stable than the empty Minkowskian space-time solution. Thus, it is worth noting that this configuration of fields might serve, under further specific conditions chosen for the particular physical system [24], as the background one. It appears in equations of motions of all new fields that enter into the system weakly [24]. This suggests that configurations similar to the obtained self-consistent gravito-dilatonic one could be the main building materials for the observed structures in the universe, both on the microscopic [24] and, as it is suggested below, on the astrophysical and cosmological scales, too.

2.2. The problems of the space-time singularity and Kaluza-Klein type excitations

Firstly, in Section 4.2 as far as the space-time geometry is discussed, it will be proven that the space-time singularity connected with the metric tensor (28) is the one through

which only the null geodesics could pass through. Hence, the obtained solution is not in contradiction with “cosmic censorship”, a conjecture that is still not proven [48].

Secondly, the problem to discuss is the Kaluza-Klein type excitations. In general, in the Kaluza-Klein gravity, the ground state solutions can contain a number of the resulting four-dimensional (massless or not) fields [21].

For example, into the presented model, in addition to the six-dimensional dilatonic field given by Eq.(23), two massless scalars tied with the shape of a two-dimensional internal parametric space (11) could also be incorporated [24]. Then, their existence is highly constrained by observations that usually tend to rule out the models. However, this is not the fate of our non-homogenous solution. Indeed, it was noticed in [24] that unless additional fields enter, on the level of the equations of motion (4) and (6), the theory is scale invariant (see also Section 5). Yet, when a new scalar field ϕ is introduced then the massless dilatonic field φ of the model, which is the Goldstone one, gives masses to the “undesirable” Kaluza-Klein type moduli fields. As the Goldstone mode, the dilatonic field φ is absorbed by the new scalar field ϕ introduced into the system [24]. As a result, it was proven that the obtained ground state solution of the total gravito-dilatonic and ϕ fields configuration acquires two spinorial degrees of freedom, where the origin of its non-zero spin is perceived as a manifestation of both the geometry of the internal two-dimensional parametric space (11) and of the kinematics of the field ϕ inside it. The obtained configuration can be interpreted as, e.g. the neutron (but other particle solutions are possible also) [24]. Therefore, the model can be extended in such a way that the intrinsic geometrical and kinematical properties of fields in the extra dimensions also manifest themselves in possible observational consequences in the realm of the physics of one particle. In consequence, e.g. the relevant observable neutron excited states were also calculated [24].

To secure the stability of this composite model of the neutron, it was found that the size of the parametric space has to be equal to $d \approx 0.2071$ fm [24]. This signifies the large extra dimension solution of d , which is of the substantial fraction of the nucleon size, which is evidently not excluded by the experiment [4]. Simultaneously, the inclusion of the additional scalar field ϕ does not lead to the destruction of our background dilatonic solution (23) as was argued in [24].

Finally, the problem of quantum fluctuations can also be considered. Yet, the existing quantum field theory (QFT) interpretation of all physical phenomena could and should be questioned [49] (see [53, 42, 21]), i.e. there may exist physical realities for which the existence of the quantum fluctuations is not necessary at all. Nowhere is this problem so crucial as in the case of gravitational interaction, at least as far as the experiment is considered. If this is a problem of general relativity, hence, it is also of its Kaluza-Klein gravity extensions.

In the present paper the astrophysical and cosmological significance of the solution is discussed.

Example	$M [M_\odot]$	$A [pc]$
sun	1.	$0.96 \cdot 10^{-13}$
globular cluster	$10^4 - 10^6$	$0.96 (10^{-9} - 10^{-7})$
galactic nucleus*	10^7	$0.96 \cdot 10^{-6}$
galaxy	$5 \cdot 10^{11}$	$4.79 \cdot 10^{-2}$
binary galaxy system*	$1 \cdot 10^{15}$	$0.96 \cdot 10^2$
galaxy-quasar system*	$2 \cdot 10^{18}$	$1.91 \cdot 10^5$

Table 1. Values of the parameter A for which the six-dimensionality of the world influences the dynamics of test particles in a similar way as the existence (in the 4-dimensional world) of mass M (given for some examples motivated by astrophysics). The examples marked by * are exceptional in the sense that parameter A has been estimated due to the demand to explain the observed redshift peculiarities of such systems. Hence, the mass M has a purely effective meaning here — for details see Sections 4 and 6.

3. Some properties of solutions

If the parameter A is strictly positive, $A > 0$, then Eqs.(21)-(23) are valid for all $r > 0$. (*The discussion of $A < 0$ case will be left for Appendix A.*) The metric tensor becomes singular only at $r = 0$; nevertheless, its determinant g (see Eq.(29)) remains well defined. Below, several formulae which will be useful in the later discussion are collected. We start with time and the radial components of the metric g_{MN} and the internal “radius” $\varrho(r)$ (see Eqs.(22) and (28))

$$\begin{cases} g_{tt} = \frac{r}{r+A} \\ g_{rr} = -\frac{r}{r+A} \\ \varrho(r) = d\sqrt{\frac{r+A}{r}} \end{cases} . \quad (36)$$

It will be also useful to write the explicit relation for the real, physical radial distance r_l from the center

$$r_l = \int_0^r dr \sqrt{-g_{rr}} = \sqrt{\frac{r}{r+A}} (r+A) + \frac{1}{2} A \ln\left(\frac{A}{A+2r+2(r+A)\sqrt{\frac{r}{r+A}}}\right) < r . \quad (37)$$

Note: Let us recall that in the standard derivation of the Schwarzschild solution, the free parameter in the metric tensor is identified with the total mass of a spherically symmetric configuration due to the demand that at large distances the metric tensor should reproduce the Newtonian potential. Because $g_{tt} \rightarrow 1$ for $r \rightarrow \infty$ (see Eq.(36)), it is interesting to compare the gravitational potential $g_{tt} = \frac{r}{r+A} \approx 1 - \frac{A}{r}$ for $r \gg A$ with the gravitational potential $g_{tt} = 1 - \frac{G}{c^2} \frac{2M}{r}$, which is induced by a mass M in the Newtonian limit. G and c are the four-dimensional gravitational constant and the velocity of light, respectively. Comparing these two potentials, we obtain that $A = 2\frac{G}{c^2}M$, so parameter A can have similar dynamical consequences as the mass M . (*The dynamical interpretations of A are different for other powers of $\frac{A}{r}$.*) Table 1 contains some astrophysically interesting masses that mimic the values of parameter A .

In this case, the gravitational potential g_{tt} (see Eq.(28) or Eq.(36)) is attractive although there is no massive matter acting as a source. Nevertheless, we cannot essentially identify parameter A directly with M . The reason is that the presented solution describes a case where ordinary matter is absent and the (only) contribution to the energy-momentum tensor comes from the infinitely stretched, massless dilatonic field φ .

It is well known [54] that the frequency ω_0 of light, moving along the geodesic line in a gravitational field that is static or stationary and measured in units of time t , is constant ($\omega_0 = \text{constant}$) along the geodesic. The frequency ω of light as a function of the proper time τ ($d\tau = \sqrt{g_{tt}} dt$) is equal to

$$\omega = \omega_0 \frac{dt}{d\tau} = \frac{\omega_0}{\sqrt{g_{tt}}} = \omega_0 \sqrt{g^{tt}} . \quad (38)$$

Let us assume that a photon with frequency ω_σ (measured in units of the proper time τ) is emitted from a source that is located at a point $r = r_\sigma$ where $g_{tt} = g_{tt}^\sigma$. Then the photon is moving along a geodesic line that reaches the observer (*obs*) at the point $r = r_{obs}$, where $g_{tt} = g_{tt}^{obs}$, with the frequency ω_{obs}

$$\frac{\omega_{obs}}{\omega_\sigma} = \sqrt{\frac{g_{obs}^{tt}}{g_\sigma^{tt}}} = \sqrt{\frac{g_{tt}^\sigma}{g_{tt}^{obs}}} . \quad (39)$$

Using Eq.(36) we can rewrite Eq.(39) as

$$\frac{\omega_{obs}}{\omega_\sigma} = \frac{\sqrt{\frac{r_\sigma}{r_\sigma + A}}}{\sqrt{\frac{r_{obs}}{r_{obs} + A}}} . \quad (40)$$

For simplicity, let us consider a limiting case in which the observer is situated at infinity. Then we get

$$\frac{\omega_{obs}}{\omega_\sigma} = \sqrt{\frac{r_\sigma^w}{r_\sigma^w + 1}} , \quad \text{where} \quad r_\sigma^w = \frac{r_\sigma}{A} . \quad (41)$$

Therefore, we see that the nearer the source is to the center of the field $\varphi(r)$ the more the emitted photon is redshifted at the point where it reaches the observer. It should also be emphasized that this redshift does depend on the relative radius $r^w = \frac{r}{A}$ rather than separately on r and A (see also Section 5).

4. Six-dimensional Hamilton-Jacobi equation for a “test particle”

In order to gain a better understanding concerning possible manifestations of the six-dimensionality of the world, let us investigate the motion of a “test particle” of mass m in the central gravitational field described by Eq.(28). Whether the moving object can be treated as a “test particle” depends on the value of parameter A in the metric tensor g_{MN} (see Eq.(28)).

The Hamilton-Jacobi equation

$$g^{MN} \partial_M S \partial_N S - m^2 c^2 = 0 \quad (42)$$

describing the motion of a test particle reads

$$\begin{aligned} & \frac{r+A}{r} \left(\frac{\partial S}{c \partial t} \right)^2 - \frac{r+A}{r} \left(\frac{\partial S}{\partial r} \right)^2 - \frac{1}{r^2} \left(\frac{\partial S}{\partial \Theta} \right)^2 - \frac{1}{r^2 \sin^2 \Theta} \left(\frac{\partial S}{\partial \Phi} \right)^2 \\ & - \frac{1}{d^2} \frac{r}{r+A} \frac{1}{\cos^2 \vartheta} \left(\frac{\partial S}{\partial \vartheta} \right)^2 - \frac{1}{d^2} \frac{r}{r+A} \left(\frac{\partial S}{\partial \zeta} \right)^2 - m^2 c^2 = 0, \end{aligned} \quad (43)$$

where S denotes the complete integral of the Hamilton-Jacobi equation and m is the mass of a “test particle” in six-dimensional space-time.

Without loss of generality, we shall restrict ourselves to the motion in the plane $\Theta = \pi/2$, thus

$$\frac{\partial S}{\partial \Theta} = 0. \quad (44)$$

If the integral S depends on a non-additive constant, which is the energy \mathcal{E}_0 (the Hamiltonian does not depend explicitly on time), then the standard procedure of the separation of variables begins with the following factorization of S

$$S = -\mathcal{E}_0 t + \mathcal{M}_\Phi \Phi + S_r(r) + \mathcal{M}_\zeta \zeta + S_\vartheta(\vartheta). \quad (45)$$

The separation constants \mathcal{E}_0 , \mathcal{M}_Φ and \mathcal{M}_ζ have the meaning of the total energy, the effective angular momentum and the internal angular momentum, respectively. Then by separating Eq.(43) into four-dimensional and internal parts, one arrives at the formula

$$\begin{aligned} & \frac{r+A}{r} \left[\frac{r+A}{r} \left(\frac{\mathcal{E}_0}{c} \right)^2 - \frac{r+A}{r} \left(\frac{\partial S_r}{\partial r} \right)^2 - \frac{1}{r^2 \sin^2 \Theta} \mathcal{M}_\Phi^2 - m^2 c^2 \right] \\ & = \frac{1}{d^2} \frac{1}{\cos^2 \vartheta} \left(\frac{\partial S_\vartheta}{\partial \vartheta} \right)^2 + \frac{1}{d^2} \mathcal{M}_\zeta^2 =: k_{\vartheta\zeta}^2 = \text{constant}. \end{aligned} \quad (46)$$

The last equation in (46) is easy to integrate for S_ϑ

$$S_\vartheta = \pm (d^2 k_{\vartheta\zeta}^2 - \mathcal{M}_\zeta^2)^{\frac{1}{2}} \sin \vartheta =: \pm k_\vartheta d \sin \vartheta, \quad (47)$$

where k_ϑ has the meaning of the internal momentum and one can distinguish the square of the (total) internal momentum $k_{\vartheta\zeta}^2$

$$k_{\vartheta\zeta}^2 = \frac{\mathcal{M}_\zeta^2}{d^2} + k_\vartheta^2. \quad (48)$$

Finally, the quantity

$$m_4^2 = m^2 + \frac{k_{\vartheta\zeta}^2}{c^2} \quad (49)$$

in Eq.(46) can be interpreted as the four-dimensional square mass of a test particle in the flat Minkowskian limit at infinity. In the case of the vanishing internal momentum $k_{\vartheta\zeta} = 0$, the four and six-dimensional masses are equal $m_4 = m$. If the six-dimensional mass is zero $m = 0$, then the four-dimensional mass at spatial infinity would be solely of an internal origin: $m_4 = \frac{|k_{\vartheta\zeta}|}{c}$.

Now, let us consider the radial part $S_r(r)$, which can easily be read from Eq.(46)

$$\frac{dS_r}{dr} = \left[\frac{\mathcal{E}_0^2}{c^2} - \left(m^2 c^2 + \frac{\mathcal{M}_\Phi^2}{r^2} \right) \frac{r}{r+A} - k_{\vartheta\zeta}^2 \left(\frac{r}{r+A} \right)^2 \right]^{\frac{1}{2}},$$

which after formal integration gives

$$S_r(r) = \int dr \left[\frac{\mathcal{E}_0^2}{c^2} - \left(m^2 c^2 + \frac{\mathcal{M}_\Phi^2}{r^2} \right) \frac{r}{r+A} - k_{\vartheta\varsigma}^2 \left(\frac{r}{r+A} \right)^2 \right]^{\frac{1}{2}}.$$

The trajectory of a test particle is implicitly determined by the following equations

$$\frac{\partial S}{\partial \mathcal{E}_0} = \alpha_1 = -t + \frac{\partial S_r(r)}{\partial \mathcal{E}_0}, \quad (50)$$

$$\frac{\partial S}{\partial \mathcal{M}_\Phi} = \alpha_2 = \Phi + \frac{\partial S_r(r)}{\partial \mathcal{M}_\Phi}, \quad (51)$$

where α_1 and α_2 are constants and without loss of generality, the initial conditions can be chosen so that $\alpha_1 = \alpha_2 = 0$. In other words, integration of Eq.(51) gives the trajectory $r = r(\Phi)$ of a test particle and Eq.(50) provides the temporal dependence of radial coordinate $r = r(t)$. These two relations determine the trajectory $r = r(t)$ and $\Phi = \Phi(t)$ of a test particle [55].

Implementing the above outlined procedure, we obtain (from Eq.(50) and Eq.(50))

$$t = \frac{\mathcal{E}_0}{c^2} \int dr \left[\frac{\mathcal{E}_0^2}{c^2} - \left(m^2 c^2 + \frac{\mathcal{M}_\Phi^2}{r^2} \right) \frac{r}{r+A} - k_{\vartheta\varsigma}^2 \left(\frac{r}{r+A} \right)^2 \right]^{-\frac{1}{2}} \quad (52)$$

and consequently the radial velocity

$$\frac{dr}{dt} = \frac{c^2}{\mathcal{E}_0} \left[\frac{\mathcal{E}_0^2}{c^2} - \left(m^2 c^2 + \frac{\mathcal{M}_\Phi^2}{r^2} \right) \frac{r}{r+A} - k_{\vartheta\varsigma}^2 \left(\frac{r}{r+A} \right)^2 \right]^{\frac{1}{2}}. \quad (53)$$

It is easy to note that the quantity

$$m_4(r) = \sqrt{m^2 \left(\frac{r}{r+A} \right) + \frac{k_{\vartheta\varsigma}^2}{c^2} \left(\frac{r}{r+A} \right)^2} \quad (54)$$

can be interpreted as the mass in four-dimensional curved space-time. The mass m_4 in Eq.(49) is recovered as the limit of $m_4(r)$ for $r \rightarrow \infty$. Similar to our previous discussion, if $k_{\vartheta\varsigma} = 0$ then $m_4(r) = m \sqrt{\frac{r}{r+A}}$ and if $m = 0$ then the mass $m_4(r)$ would have an internal origin $m_4(r) = \frac{|k_{\vartheta\varsigma}|}{c} \left(\frac{r}{r+A} \right)$. It should also be emphasized that $m_4(r)$ does depend on the ratio $r^w = \frac{r}{A}$ rather than separately on r and A , which is a reflection of the scale-invariance of the model (see also Section 5 and [24]).

Let us also notice that the non-negativity of the square of the four-dimensional mass $m_4^2(r) \geq 0$ gives the first condition on the value of $k_{\vartheta\varsigma}^2$

$$m_4^2(r) \geq 0, \quad \text{so} \quad k_{\vartheta\varsigma}^2 \geq k_{\vartheta\varsigma m_4}^2 \equiv -c^2 m^2 \frac{(r+A)}{r}. \quad (55)$$

If the entire spacelike hypersurface is to be accessible for a particle, then from the validity of the condition $m_4^2(r) \geq 0$, the condition $k_{\vartheta\varsigma}^2 \geq -m^2 c^2$ follows. Otherwise, Eq.(55) is the condition for the maximum value of the radius r

$$r \leq r^{max} \equiv r^{max}(k_{\vartheta\varsigma m_4}^2) \equiv -A / \left(1 + \frac{k_{\vartheta\varsigma m_4}^2}{m^2 c^2} \right). \quad (56)$$

It may appear strange that $k_{\vartheta\varsigma}^2 \geq -m^2 c^2$ by which some imaginary values of $k_{\vartheta\varsigma}$ are also allowed. However, one should not uncritically transfer from four-dimensional intuitions (such like $k_{\vartheta\varsigma}^2 \geq 0$ or $m^2 \geq 0$, although some of them may turn out to be true) to e.g. the six-dimensional one but rather build on the safe ground of known properties of four-dimensional sector i.e. $m_4^2 \geq 0$ in this case [14].

Now, using the Eq.(51) and Eq.(50) we obtain

$$\Phi = \int \left[\frac{\mathcal{E}_0^2}{c^2} - \left(m^2 c^2 + \frac{\mathcal{M}_\Phi^2}{r^2} \right) \frac{r}{r+A} - k_{\vartheta\varsigma}^2 \left(\frac{r}{r+A} \right)^2 \right]^{-\frac{1}{2}} \frac{\mathcal{M}_\Phi dr}{r(r+A)} \quad (57)$$

and consequently using Eqs.(57) and (53), the angular velocity of the particle reads

$$\Omega_t = \frac{d\Phi}{dt} = \frac{dr}{dt} \frac{d\Phi}{dr} = \frac{c^2 \mathcal{M}_\Phi}{\mathcal{E}_0 r (r+A)} \quad (58)$$

Now, the proper angular velocity of the particle is equal to

$$\Omega_\tau = \frac{d\Phi}{d\tau} = \Omega_t \sqrt{\frac{r+A}{r}}, \quad (59)$$

where τ is the proper time and $d\tau = \sqrt{g_{tt}} dt$ (where g_{tt} is as in Eq.(28)).

The transversal velocity of the particle (i.e. the component perpendicular to the radial direction) is equal to (see Eq.(37))

$$v_t = \Omega_t r_l \quad (60)$$

and analogously, the transversal component of the proper velocity (written in the units of the proper time τ) is equal to

$$v_\tau = \Omega_\tau r_l = v_t \sqrt{\frac{r+A}{r}} \quad (61)$$

where Ω_t , Ω_τ and r_l are given by Eqs.(58),(59) and (37), respectively.

Let us rewrite Eq.(53) in the following form

$$\frac{dr}{dt} = \frac{c}{\mathcal{E}_0} \sqrt{\mathcal{E}_0^2 - \mathcal{U}_{eff}(r)} \quad (62)$$

where

$$\mathcal{U}_{eff}(r) = \left[\left(m^2 c^4 + \left(\frac{\mathcal{M}_\Phi}{r} \right)^2 c^2 \right) \frac{r}{r+A} + (k_{\vartheta\varsigma}^2 c^2) \left(\frac{r}{r+A} \right)^2 \right]^{\frac{1}{2}} \quad (63)$$

The function $\mathcal{U}_{eff}(r)$ plays the role of effective potential energy in the meaning that the relation between \mathcal{E}_0 and $\mathcal{U}_{eff}(r)$ determines the allowed regions of the motion of the particle.

The proper radial velocity of the particle is equal to

$$v_r = \frac{dr_l}{d\tau} = \frac{\sqrt{-g_{rr}} dr}{\sqrt{g_{tt}} dt} = \frac{dr}{dt}, \quad (64)$$

where in the last equality the relation $g_{tt} = -g_{rr}$ is used (see Eq.(36)). So the radial velocity dr/dt and the proper radial velocity $v_r = dr_l/d\tau$ are equal, and one should stress that this property is fundamentally different from the analogous relation for a black hole.

4.1. Stable circular orbits.

Let us consider for $A > 0$ a stable circular orbit with given values of \mathcal{E}_0 , \mathcal{M}_Φ and $k_{\vartheta\varsigma}$. The radius of this orbit can be calculated from the following equations (see Eqs.(62), (63),(64))

$$\frac{dr}{dt} = 0, \quad (65)$$

$$\frac{dv_r}{dt} = \frac{d^2r}{dt^2} = \frac{dr}{dt} \frac{d}{dr} \left(\frac{dr}{dt} \right) = 0. \quad (66)$$

From Eqs.(66),(62),(63) we obtain the implicit relation between the radius r_s of the stable circular orbit (index s), the angular momentum of the particle \mathcal{M}_Φ and the internal ‘‘total momentum’’ $k_{\vartheta\varsigma}$

$$(\mathcal{M}_\Phi)^2 = \left(m^2 c^2 + 2 k_{\vartheta\varsigma}^2 \left(\frac{r_s}{r_s + A} \right) \right) \left(\frac{A}{2 r_s + A} \right) r_s^2 \quad (67)$$

so

$$\mathcal{M}_\Phi = \pm A^{1/2} r_s \sqrt{\frac{(r_s + A) m^2 c^2 + 2 k_{\vartheta\varsigma}^2 r_s}{A^2 + 3 A r_s + 2 r_s^2}}. \quad (68)$$

It is easy to verify that because $k_{\vartheta\varsigma} = \text{const}$, hence $\mathcal{M}_\Phi/r_s \rightarrow 0$ as r_s tends to infinity. Using Eqs.(65),(62), (63) we calculate the total energy \mathcal{E}_0 of a particle moving along the stable circular orbit of the radius r_s

$$(\mathcal{E}_0)^2 = \left[m^2 c^4 + \left(m^2 c^4 + 2 k_{\vartheta\varsigma}^2 c^2 \frac{r_s}{r_s + A} \right) \frac{A}{2 r_s + A} \right] \left(\frac{r_s}{r_s + A} \right) + k_{\vartheta\varsigma}^2 c^2 \left(\frac{r_s}{r_s + A} \right)^2 \quad (69)$$

or in other words

$$\mathcal{E}_0 = c^2 \sqrt{\frac{r_s [2 (r_s + A)^2 m^2 c^2 + 3 A r_s k_{\vartheta\varsigma}^2 + 2 r_s^2 k_{\vartheta\varsigma}^2]}{c^2 (r_s + A)^2 (2 r_s + A)}}. \quad (70)$$

As the first example, let us consider the motion of a particle with given values of $\mathcal{M}_\Phi \neq 0$ and $k_{\vartheta\varsigma}$. Figure 1 illustrates the function $\mathcal{U}_{eff}(r)$ for different values of \mathcal{M}_Φ and $k_{\vartheta\varsigma} = 0$.

Similarly, Figure 2 shows the function $\mathcal{U}_{eff}(r)$ for different values of $k_{\vartheta\varsigma}$ with a fixed value of \mathcal{M}_Φ .

For the particular system r_s is established and $k_{\vartheta\varsigma}$ is the constant of motion. Yet, there are some physically obvious conditions which in turn restrict admissible values of the radii of stable orbits for a given internal momentum $k_{\vartheta\varsigma}$. Namely, from Eq.(67) we obtain

$$(\mathcal{M}_\Phi)^2 > 0, \quad \text{so} \quad k_{\vartheta\varsigma}^2 > k_{\vartheta\varsigma\mathcal{M}_\Phi}^2, \quad (71)$$

where

$$k_{\vartheta\varsigma\mathcal{M}_\Phi}^2 \equiv - \frac{m^2 c^2}{2} \left(\frac{r_s + A}{r_s} \right) \quad (72)$$

and from Eq.(69) we obtain

$$(\mathcal{E}_0)^2 \geq 0, \quad \text{so} \quad k_{\vartheta\varsigma}^2 \geq k_{\vartheta\varsigma\mathcal{E}_0}^2, \quad (73)$$

where

$$k_{\vartheta\zeta\mathcal{E}_0}^2 \equiv -m^2 c^2 \frac{2(r_s + A)}{2r_s + 3A} \left(\frac{r_s + A}{r_s} \right) < -m^2 c^2. \quad (74)$$

It is easy to verify that condition (71)-(72) is stronger than (73)-(74) which in turn is the one that is stronger than (55), that is

$$k_{\vartheta\zeta}^2 > k_{\vartheta\zeta\mathcal{M}_\Phi}^2 > k_{\vartheta\zeta\mathcal{E}_0}^2 > k_{\vartheta\zeta m_4^2}^2, \quad (75)$$

which means that the stability condition of the system is guaranteed by the first inequality in (75), i.e. by the condition (71)-(72). Now, let us calculate the proper angular velocity and the proper transversal velocity of a particle moving along the stable circular orbit determined by Eqs.(65),(66). Using Eqs.(58)-(61) with \mathcal{M}_Φ and \mathcal{E}_0 given by Eq.(68) and Eq.(70), respectively, we obtain the proper angular velocity

$$\Omega_\tau^s = \frac{c^2 \mathcal{M}_\Phi}{\mathcal{E}_0 r_s (r_s + A)} \sqrt{\frac{r_s + A}{r_s}} \quad (76)$$

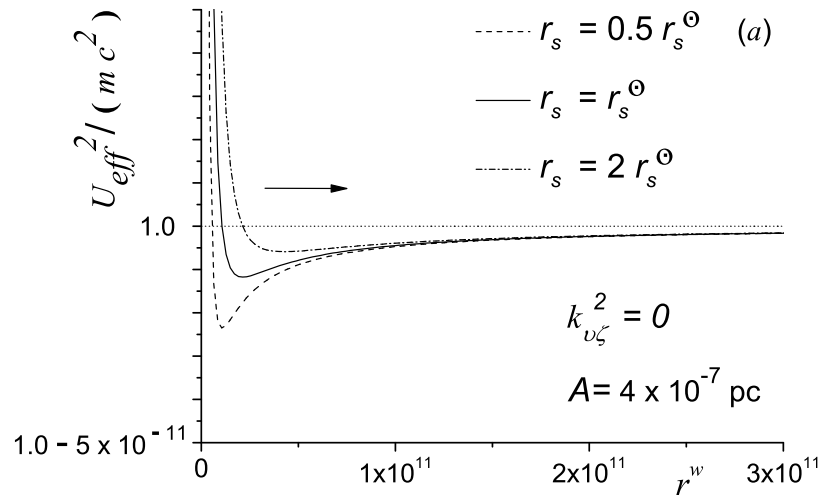


Figure 1. The potential \mathcal{U}_{eff} (in units of mc^2) (see Eq.(63)) for $k_{\vartheta\zeta}^2 = 0$ and different values of \mathcal{M}_Φ as a function of the relative radius $r^w = r/A$. Horizontal arrow above the curves, consistent with moving of the minimum of \mathcal{U}_{eff} to the right, denotes the direction of the increasing angular momentum \mathcal{M}_Φ . The minimum of the potential \mathcal{U}_{eff} determines the radius r_s^w , and hence the value of $r_s = r_s^w A$ of the stable circular orbit (index s). The radii r_s^w of stable orbits corresponding to the minima of the potentials depicted on Figure 1 are $1.0625 \cdot 10^{10}$, $2.125 \cdot 10^{10}$ and $4.25 \cdot 10^{10}$, respectively. The middle curve (solid line) illustrates the effective potential for the stable circular orbit with a radius equal to the distance of the sun from the center of the dilatonic field φ (with the parameter A equal to $4 \cdot 10^{-7}$ pc) located at the center of the Milky Way, i.e. $r_s^\odot = 8.5$ kpc.

and the proper tangent velocity of the particle

$$v_\tau^s = \frac{c^2 \mathcal{M}_\Phi}{\mathcal{E}_0 \sqrt{r_s (r_s + A)}} \frac{r_{ls}}{r_s}, \quad (77)$$

where r_{ls} is given by Eq.(37) for the stable circular orbit. Looking at Eqs.(68),(70), it is not difficult to notice that v_τ^s again depends on the ratio $r_s^w = \frac{r_s}{A}$ rather than on r_s and A independently.

From Eq.(77) and Eqs.(68),(70) and for $m \neq 0$, one can notice that if

$$k_{\vartheta\zeta}^2 \propto \mathcal{C} \cdot m^2, \quad \text{where } \mathcal{C} = \text{constant} \quad (78)$$

then v_τ^s does not depend explicitly on the mass m of the particle. However, unless the relation between the proportionality constant \mathcal{C} and the square of the velocity of light c is not unique, from Eqs.(77), (68) and (70), it can be noticed that v_τ^s is additionally parameterized by \mathcal{C} . This is clearly the non-classical effect that influences the shape of the rotation curves (Figure 3). The only bounds on \mathcal{C} that arise in the model follow from the constraints of causality [14] (55), energy (73)-(74) and angular momentum (71)-(72) analyzed above. For example, the angular momentum constraint (71)-(72) fulfilled on the entire spacelike hypersurface gives, according to Eq.(78), the condition $\mathcal{C} > \mathcal{C}_{bound}$ with the lowest bound $\mathcal{C}_{bound} = -c^2/2$ on which $k_{\vartheta\zeta}^2/(c^2 m^2) = -1/2$, so that the internal momentum $k_{\vartheta\zeta}$ fulfills the relation $k_{\vartheta\zeta}^2/(c^2 m^2) > k_{\vartheta\zeta}^2/(c^2 m^2) = -1/2$. Although it is not excluded, we do not yet know the rule that forces the proportionality

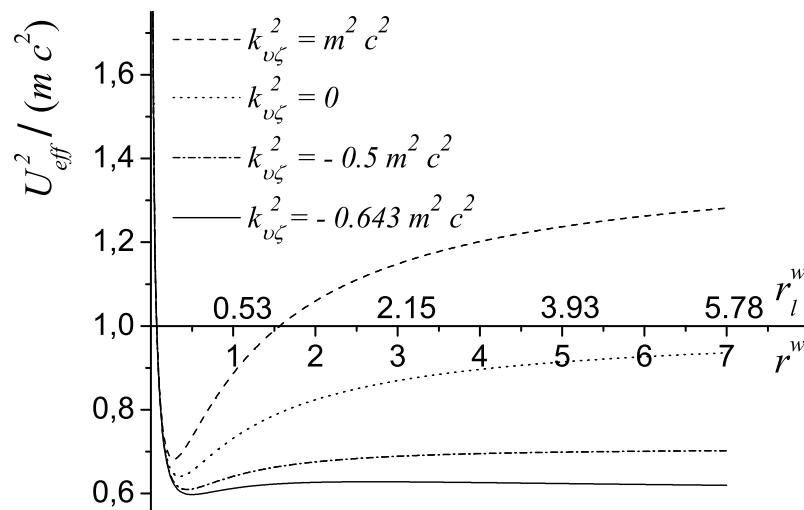


Figure 2. The potential \mathcal{U}_{eff} (in units of mc^2) (see Eq.(63)) for different values of $k_{\vartheta\zeta}$ as a function of the relative radius $r^w = r/A$. For all curves, the value $\mathcal{M}_\Phi/A = 0.267 mc$ is chosen. This value of \mathcal{M}_Φ/A is the one for the angular momentum of a particle on the stable orbit (the minimum of \mathcal{U}_{eff}) with $k_{\vartheta\zeta}^2 = -0.643 m^2 c^2$ for which the radius is equal to $r_s^w = 1/2$ (solid line). In this case (solid line), the maximum of \mathcal{U}_{eff} is at the finite radius equal to $r^w \approx 2.69$.

constant \mathcal{C} in Eq.(78) to be the same for all test particles inside the configuration with the particular central dilatonic field φ .

Finally, if (phenomenologically) \mathcal{C} in Eq.(78) is scaled with r_s , then the profile of the proper tangent velocity v_τ^s given by Eq.(77), and thus the rotation curves, could be modified. The systematic determination of such a rule fulfilled by \mathcal{C} lies beyond the analysis of this paper.

4.1.1. The case with $m \neq 0$. From Eqs.(71)-(72) we notice that if $k_{\vartheta\varsigma}^2 > -\frac{1}{2}m^2c^2$ then all values of the radius r_s (or r_{ls} , see Eq.(37)) for stable orbits are allowed. Figure 3 displays the rotation curves calculated according to Eq.(77) (in units of the velocity of light c) for different values of $k_{\vartheta\varsigma}^2$. It shows that the whole effect is i) most pronounced in the region close to the center of the spherically symmetric configuration of the dilatonic field φ and is, ii) except for the case of $k_{\vartheta\varsigma}^2 < -\frac{1}{2}m^2c^2$ discussed below, extended from the center to the infinity. For example, let us take the sun in the Milky Way. Then, e.g. for $k_{\vartheta\varsigma} = 0$ and at the distance of $r_s^\odot = 8.5$ kpc from the center of the dilatonic field φ that is overlapping with the center of the Milky Way, we obtain the contribution of v_τ^s (caused by the dilatonic field φ with the parameter A equal to $4 \cdot 10^{-7}$ pc) to the total proper tangent velocity equal to 1.45 km/s.

If, however,

$$k_{\vartheta\varsigma,min}^2 \equiv k_{\vartheta\varsigma,\mathcal{M}_\Phi}^2 < k_{\vartheta\varsigma}^2 < -\frac{1}{2}m^2c^2 \quad (79)$$

then according to Eqs.(71)-(72), the radius of the stable circular orbits has to fulfill the relation

$$r_s < r_s^{max}, \quad (80)$$

where the limiting value is equal to

$$r_s^{max} \equiv r_s^{max}(k_{\vartheta\varsigma,\mathcal{M}_\Phi}^2) \equiv -A/(1 + \frac{2k_{\vartheta\varsigma,\mathcal{M}_\Phi}^2}{m^2c^2}). \quad (81)$$

In other words, the condition (71)-(72) implies that one cannot find any stable orbit with $r_s > r_s^{max}$ for a fixed $k_{\vartheta\varsigma}^2$, which is from the range given by Eq.(79) and with the angular momentum \mathcal{M}_Φ chosen according to Eq.(68). In this case, the orbit with $r_s = r_s^{max}$ is the metastable one. For the limiting value, i.e. for $k_{\vartheta\varsigma}^2 = -\frac{1}{2}m^2c^2$ we can notice that $r_s^{max} \rightarrow \infty$.

Note: Above, we have seen that (for $m \neq 0$) $k_{\vartheta\varsigma}^2 = k_{\vartheta\varsigma,\mathcal{M}_\Phi}^2 \equiv -\frac{1}{2}m^2c^2$ is the boundary between configurations of test particles having stable orbits on the entire spacelike hypersurface and configurations with unstable orbits beginning with the radius r_s^{max} and upwards. Interestingly, in accordance with Eq.(48), we can also notice that if the value $k_{\vartheta\varsigma}^2 = -\frac{1}{2}m^2c^2$ is not to appear in the result of the accidental cancellation, then the square of the internal momentum k_ϑ and the internal angular momentum have to take one of the discrete possibilities, e.g.

$$\left(\frac{k_\vartheta}{mc}\right)^2 = -j^2 + \left(\frac{k_{\vartheta\varsigma}}{mc}\right)^2 \quad \text{and} \quad \frac{\mathcal{M}_\varsigma}{mcd} = j, \quad j = 0, \frac{1}{2}, 1, \frac{3}{2}, 2, \dots, \quad (82)$$

respectively, where $\left(\frac{k_{\vartheta\zeta}}{m c}\right)^2 = -1/2$ for the boundary stable configuration. Yet, this choice also agrees with the axial symmetry of the internal space (11) around the ϑ axis (compare also [24]).

4.1.2. *A case with $m = 0$ and $k_{\vartheta\zeta}^2 \neq 0$.* In the case of $m = 0$ and $k_{\vartheta\zeta}^2 \neq 0$, we can see from Eqs.(71)-(72),(67) and Eqs.(73)-(74),(69) that $k_{\vartheta\zeta}^2 > 0$ and all values of the radius r_s of stable orbits are allowed.

4.2. *Radial trajectories, $\mathcal{M}_\Phi = 0$.*

In this case, we investigate the free motion of a test particle (with given $k_{\vartheta\zeta}^2$) along the geodesic $\Phi = \text{constant}$ that crosses the center of the gravitational field g_{MN} . Hence, unless it is stated differently, $\mathcal{M}_\Phi = 0$ in almost all of Section 4.2. From Eqs.(64) and

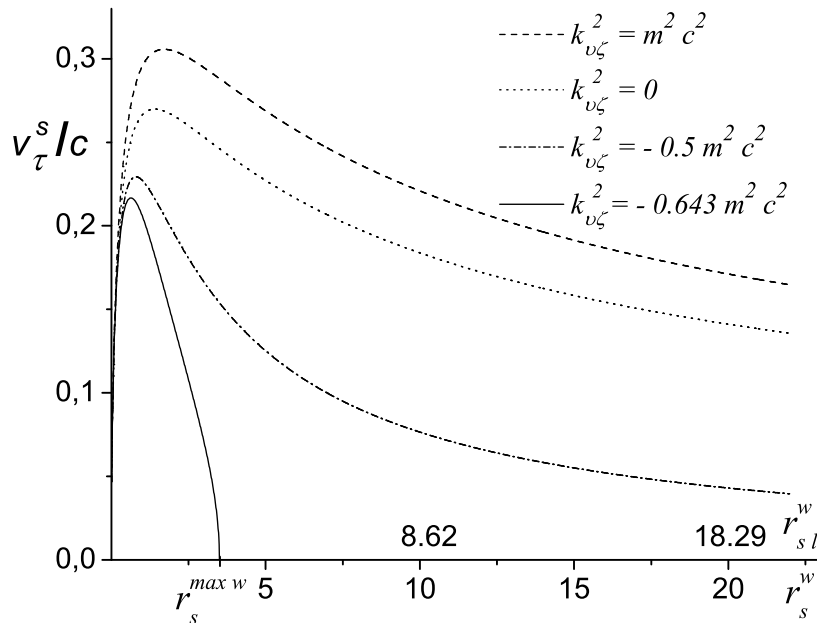


Figure 3. The proper transversal velocity v_τ^s (see Eq.(77)) of a test particle (in units of the velocity of light c) moving along a stable circular orbit determined by Eqs.(65),(66) as the function of the relative radius $r_s^w = r_s/A$ for different (but fixed for each curve) value of $k_{\vartheta\zeta}^2$ and the angular momentum \mathcal{M}_Φ calculated according to Eq.(68). If $k_{\vartheta\zeta}^2 > -\frac{1}{2} m^2 c^2$ then all values of the radius r_s^w (or $r_{sl}^w = r_{sl}/A$ cf. Eq.(37)) of stable orbits are allowed. If $k_{\vartheta\zeta, \min}^2 < k_{\vartheta\zeta}^2 < -\frac{1}{2} m^2 c^2$, then the stable orbits, for fixed $k_{\vartheta\zeta}^2$ and angular momentum \mathcal{M}_Φ chosen according to Eq.(68), may exist only to the radius $r_s^{\max, w}$ (see Eqs.(80)-(81)). If $k_{\vartheta\zeta}^2 = -0.643 m^2 c^2$ (as in Figure 2 for the solid line) then $r_s^{\max, w} \approx 3.5$ and for $r_s^w \geq r_s^{\max, w}$ there are no stable orbits. For the limiting case $k_{\vartheta\zeta}^2 = -\frac{1}{2} m^2 c^2$ we obtain $r_s^{\max, w} \rightarrow \infty$.

(62),(63), we obtain

$$v_r = \frac{c}{\mathcal{E}_0} \sqrt{\mathcal{E}_0^2 - (m^2 c^4) \frac{r}{r+A} - k_{\vartheta\varsigma}^2 c^2 \left(\frac{r}{r+A}\right)^2}. \quad (83)$$

From this we may notice that for a particle which is initially ($t = t_o$) at rest ($v_r = v_{r_o} = 0$) at the point $r = r_o \neq 0$, the total energy is equal to (compare Eq.(54))

$$\mathcal{E}_0 = \sqrt{m^2 c^4 \left(\frac{r_o}{r_o + A}\right) + k_{\vartheta\varsigma}^2 c^2 \left(\frac{r_o}{r_o + A}\right)^2} = m_4(r_o) c^2. \quad (84)$$

Therefore, the particle is oscillating and crosses the center with velocity $v_r(r=0) = c$ (at the center, the particle becomes massless $m_4(r=0) = 0$). From Eqs.(83), (53) and $d\tau = \sqrt{g_{tt}} dt$, we obtain that the acceleration of the particle is equal to

$$a_r = \frac{dv_r}{d\tau} = -A c^2 \frac{m^2 c^4 + 2 k_{\vartheta\varsigma}^2 c^2 \left(\frac{r}{r+A}\right)}{2 \mathcal{E}_0^2 (r+A)^2} \sqrt{\frac{r+A}{r}}. \quad (85)$$

4.2.1. A case with $m \neq 0$. From Eq.(85) we see that the acceleration tends to minus infinity at the center and when $k_{\vartheta\varsigma}^2 \geq -\frac{1}{2} m^2 c^2$, it monotonously increases to the zero value when r is going to infinity. So, in this case, the particle is attracted to the center for all values of r (see Figure 4).

If $-m^2 c^2 \leq k_{\vartheta\varsigma}^2 < -\frac{1}{2} m^2 c^2$ then from Eq.(85) it follows that $r = r_{a_r=0}$ with the finite value exists

$$r_{a_r=0} = -A / \left(1 + \frac{2 k_{\vartheta\varsigma}^2}{m^2 c^2}\right) \quad (86)$$

for which $a_r = 0$ (compare Eq.(81)). In this case, for $r \leq r_o < r_{a_r=0}$, the particle is attracted to the center with $a_r \rightarrow -\infty$ for $r \rightarrow 0$ and for $r \geq r_o > r_{a_r=0}$, the particle is repelled from the center and the acceleration $a_r \rightarrow 0$ when $r \rightarrow \infty$ (see Figure 4). In Figure 5 the radial acceleration a_r of the particle that is very close to the center of the field φ is presented. Because the solution is horizon free, the achieved values of acceleration of the particle could cause a visible point-like radiation (see Section 6).

4.2.2. A case with $m = 0$ and $k_{\vartheta\varsigma}^2 \neq 0$. In this case, the requirement of $\mathcal{E}_0^2 > 0$ implies $k_{\vartheta\varsigma}^2 > 0$ (see Eq.(84)). From Eqs.(83), (84) and (85), we conclude that the particle is attracted to the center ($a_r < 0$) for all values of r .

4.2.3. The causality condition. Let us suppose that we have $m_4^2(r) \geq 0$ on the entire spacelike hypersurface that is equivalent to the causality condition [14]. Hence, from (55) we see that $k_{\vartheta\varsigma}^2 \geq -m^2 c^2$ and from the formula (63), we obtain the condition for the effective potential at infinity, i.e. $\mathcal{U}_{eff}(\infty) \geq \mathcal{U}_{eff}(r=0) = 0$, with the equality if the limiting value $k_{\vartheta\varsigma}^2 = -m^2 c^2$ is chosen. With $m_4^2(r) < 0$ for $r > r^{max}$, which according to (56) is prohibited by the causality condition [14] (55), the potential $\mathcal{U}_{eff}(r)$ becomes imaginary.

4.2.4. A case with $m = 0$ and $k_{\vartheta\zeta}^2 = 0$. Now in Eq.(83) we have $\mathcal{E}_0 = \text{constant} \neq 0$ and from Eqs.(83) and (85), one can read that $v_r = c$ and $a_r = 0$ for all values of r . So, the particle which has both the six-dimensional mass m and the square of the total internal momentum $k_{\vartheta\zeta}^2$ equal to zero, which is a reasonable representation of a photon for example, does not feel (except changing the frequency according to Eq.(38)) the curvature of space-time when moving along the geodesic line crossing the center.

On the other hand, for $\mathcal{M}_\Phi \neq 0$, $m = 0$ and $k_{\vartheta\zeta}^2 = 0$, using Eq.(57) and introducing formally the parameter $r_m = \frac{\mathcal{M}_\Phi c}{\mathcal{E}_0}$, we obtain the trajectory of the particle

$$\Phi = \int \left[\frac{1}{r_m^2} - \frac{1}{r^2} \frac{r}{r+A} \right]^{-\frac{1}{2}} \frac{dr}{r(r+A)} \quad \text{for } \mathcal{M}_\Phi \neq 0. \quad (87)$$

When $A \rightarrow 0$ then the trajectory calculated according to the above equation is a straight line $r = r_m/(\sin \Phi)$ passing the center at the distance of r_m (impact parameter). On the other hand, light travelling in our space-time with $A \neq 0$ is deflected even in the absence of baryonic matter (see also [Appendix B](#) on the Pericenter shift).

Remark: We should use the eikonal equation instead of the Hamilton-Jacobi equation for $m = 0$ and $k_{\vartheta\zeta}^2 = 0$. However, a formal (technical) substitution of $r_m = \frac{\mathcal{M}_\Phi c}{\mathcal{E}_0}$ gives the same analytical result (87).

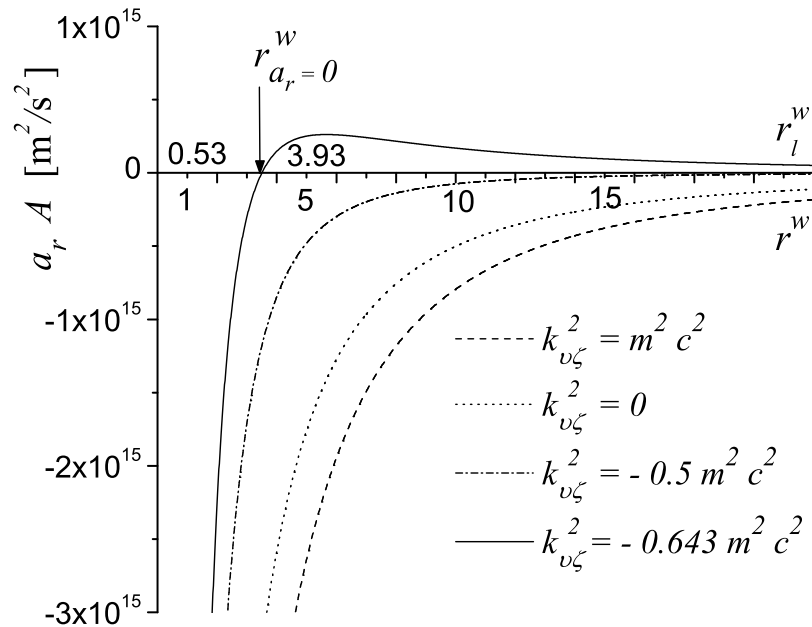


Figure 4. The acceleration a_r (in units of $1/A$) of a test particle moving along a radial trajectory (see Eq.(85)). As in Figure 2, $k_{\vartheta\zeta}^2$ for the solid line is chosen as equal to $k_{\vartheta\zeta}^2 = -0.643 m^2 c^2$. Consequently $a_r = 0$ for the relative radius $r^w \equiv r/A = r_{a_r=0}^w \approx 3.5$ (see Eq.(86)) and the “particle” is attracted to the center for all values of $r^w < r_{a_r=0}^w$ and is repelled for $r^w > r_{a_r=0}^w$ (see the text). For other curves the particle is attracted to the center ($a_r < 0$) for all values of r^w .

4.3. Redshift of radiation from stable circular orbits.

Let us suppose for simplicity's sake that the observer is located far away from the center of the system at a distance far bigger than the size of the system, so its peculiar motion with respect to the center of the system is negligibly small (see Figure 6). Let us also assume that the dynamical time scale t_{dyn} is greater than the characteristic timescale t_{obs} over which the observations are performed i.e. $t_{dyn} > t_{obs}$. In such a case, the observed motion of the ‘‘luminous particle’’ is seen only as instantaneous redshift or blueshift. If the motion of the ‘‘particle’’, which is the source, takes place along the stable circular orbit, then the kinematical Doppler shift is equal to (see Figures 6,7)

$$z_D = \sqrt{\frac{c - v_\tau^s \sin\Phi(\tau)}{c + v_\tau^s \sin\Phi(\tau)}} - 1, \quad (88)$$

where the angle $\Phi(\tau) = \int_0^\tau \Omega_\tau^s d\tau$ (see Eq.(76)) is counted from the direction to observer, i.e. $\Phi(\tau = 0) = 0$, as in Figure 6, and the proper tangent velocity v_τ^s is given by Eq.(77). Now, the gravitational redshift according to Eq.(41) is equal to (see Figure 7)

$$z_g = \frac{\lambda_{obs}}{\lambda_\sigma} - 1 = \frac{\omega_\sigma}{\omega_{obs}} - 1 = \sqrt{\frac{r_s + A}{r_s}} - 1, \quad (89)$$

where $r_\sigma = r_s$.

It is not difficult to see that the combined effect of these redshifts is as follows (see Figure 8)

$$z = (z_g + 1)(z_D + 1) - 1. \quad (90)$$

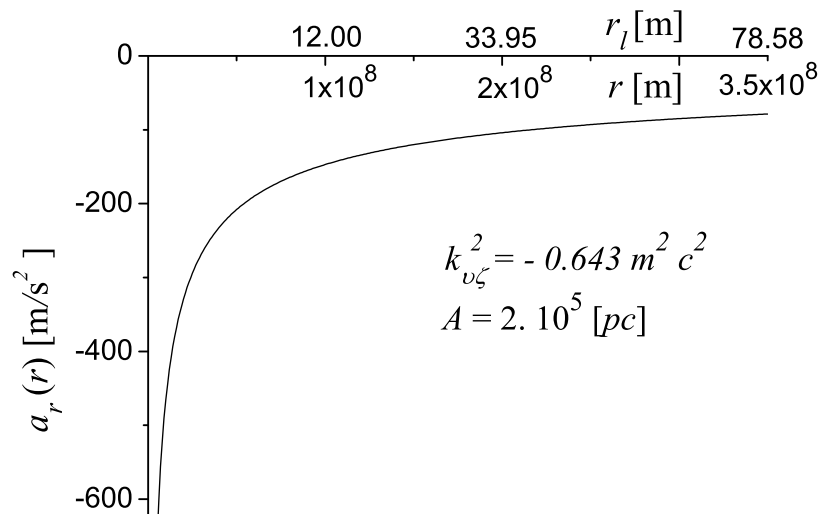


Figure 5. The radial acceleration a_r of a test particle (see Eq.(85)) for $k_{\nu\zeta}^2 = -0.643 m^2 c^2$ in the vicinity of the center of φ . The value $A = 2. 10^5$ pc was chosen as typical for quasar-galaxy systems (see Table 1 in Section 3).

For a source moving along the stable orbit away from the observer (which is at infinity), the instantaneous angle is equal to $\Phi = 3/2 \pi$ (see Figure 6) and from Eq.(88), we obtain that $z_D > 0$, i.e. the source is kinematically redshifted and the combined effect given by Eq.(90) obviously has a positive value of the redshift z (see the left-hand side of Figure 8).

In the case of the source moving towards the observer, the instantaneous angle is equal to $\Phi = \pi/2$ (see Figure 6) and $z_D < 0$, i.e. the source is kinematically bluishifted. Yet, we notice (see the right-hand side of Figure 8) that for all values of $k_{\theta\zeta}^2$, but small enough values of r_s , even in this case the combined effect given by Eq.(90) results in a positive value of the redshift z . Moreover, for sufficiently small values of $k_{\theta\zeta}^2 < -\frac{1}{2} m^2 c^2$, e.g. for $k_{\theta\zeta}^2 = -0.643 m^2 c^2$ as in Figure 8, even the whole effect of the Doppler blueshift can be hidden behind the gravitational redshift. Because there are no stable orbits for $k_{\theta\zeta}^2 = -0.643 m^2 c^2$ for $r_s^w > r_s^{max,w} \approx 3.5$ (see Eq.(81)), hence for the metastable point $r_s^{max,w}$ the breaks of the curves (with solid lines) plotted on both the right- and left-hand side of Figure 8 occur.

To summarize, for the square of the total internal momentum $k_{\theta\zeta}^2$ that fulfills relation (79), we obtain in accordance with Eqs.(80)-(81) that for all allowed stable radii of the moving source, the possible Doppler blueshift is hidden behind the gravitational redshift caused by the dilatonic central field (see Figure 8).

For example, let us choose $A = 96$ pc as the characteristic value for a system of pairs of galaxies (see 5th row in Table 1). When one of the galaxies in the pair has a four-dimensional mass equal to e.g. $m_4 \approx 3.53 \times 10^{11} M_\odot$ and a radius of its stable orbit equal to $r_s = 2000 A = 192$ kpc and $k_{\theta\zeta}^2 = -0.500235 m^2 c^2$, where $m \approx 5 \times 10^{11} M_\odot$ is the six-dimensional mass of the galaxy, then the value of its total proper tangent velocity that is equal to $v_\tau^s \approx 36.6$ km/s is obtained. The gravitational redshift (89) of the galaxy is equal to $z_g \approx 0.00025$ and the maximal value of the Doppler redshift (88)

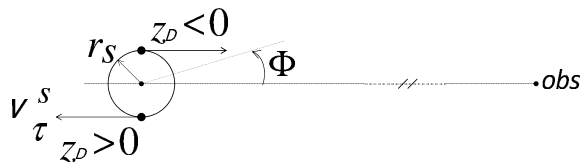


Figure 6. The Doppler shift: A source moving along the stable orbit of radius r_s . When it is moving away from the observer (which is at infinity), then the instantaneous angle is equal to $\Phi = 3/2 \pi$ and $z_D > 0$, i.e. the source is (maximally) kinematically redshifted for the observer. When the source is moving towards the observer, the instantaneous angle is equal to $\Phi = \pi/2$ and $z_D < 0$, i.e. the source is (maximally) kinematically bluishifted.

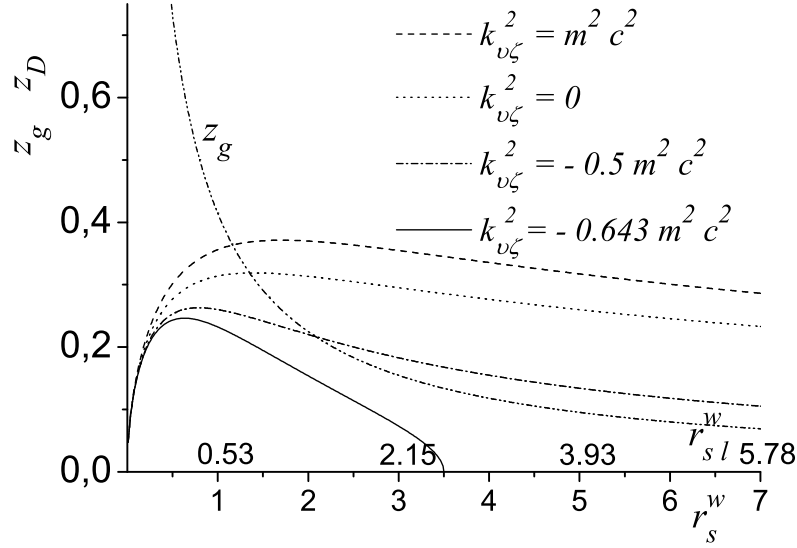


Figure 7. The (maximal) Doppler shift z_D caused by motion of the particle along a stable circular orbit (see Eq.(88)) for different values of $k_{\nu\zeta}^2$. The curve z_g denotes the gravitational redshift (see Eq.(89)).

is equal to $z_D \approx 0.00012$. Then, the combined effect of the gravitational and Doppler redshifts (see Eq.(90)) is equal to $z \approx 0.00037$ and $z \approx 0.00013$ for a galaxy moving along the stable orbit away from and towards the observer, respectively. Let us notice that, besides the huge value of (the auxiliary mass) M connected with the value of the parameter A of the gravito-dilatonic configuration (see 5th row in Table 1), the four-dimensional mass m_4 of the galaxy forms approximately 70.7% of its six-dimensional mass, which is responsible for the kinematics of the galaxy in its motion around the center of the background gravito-dilatonic field configuration. The remaining 29.3% mass is connected with the galaxy total internal momentum $k_{\vartheta\zeta}$. Thus, in some cases the mass m , which enters into the six-dimensional equations of motion could be bigger than the four-dimensional mass m_4 , which could be perceived in the four-dimensional space-time.

5. Scale invariance

Let us rewrite the Hamilton-Jacobi equation (see Eq.(43)) in the following way

$$\begin{aligned} & \frac{r^w + 1}{r^w} \left(\frac{\partial S}{\partial t^w} \right)^2 - \frac{r^w + 1}{r^w} \left(\frac{\partial S}{\partial r^w} \right)^2 - \frac{1}{(r^w)^2} \left(\frac{\partial S}{\partial \Theta} \right)^2 - \frac{1}{(r^w)^2 \sin^2 \Theta} \left(\frac{\partial S}{\partial \Phi} \right)^2 \\ & - \frac{1}{(d^w)^2} \frac{r^w}{r^w + 1} \frac{1}{\cos^2 \vartheta} \left(\frac{\partial S}{\partial \vartheta} \right)^2 - \frac{1}{(d^w)^2} \frac{r^w}{r^w + 1} \left(\frac{\partial S}{\partial \zeta} \right)^2 - (l^w c)^2 = 0, \end{aligned} \quad (91)$$

where

$$r^w = \frac{r}{A}, \quad t^w = \frac{ct}{A}, \quad d^w = \frac{d}{A}, \quad l^w = mA. \quad (92)$$

In fact Eq.(91) is scale invariant under

$$A \rightarrow \alpha A, \quad r \rightarrow \alpha r, \quad d \rightarrow \alpha d, \quad ct \rightarrow \alpha ct \quad (93)$$

only if this transformation is supplemented by

$$m \rightarrow \frac{1}{\alpha} m, \quad (94)$$

where α is the parameter of the transformation. Systems with different values of r , A , d , m and t have the same physical properties provided the values of r^w , t^w , d^w and l^w are the same. This means that whenever the dilatonic field φ is present, and

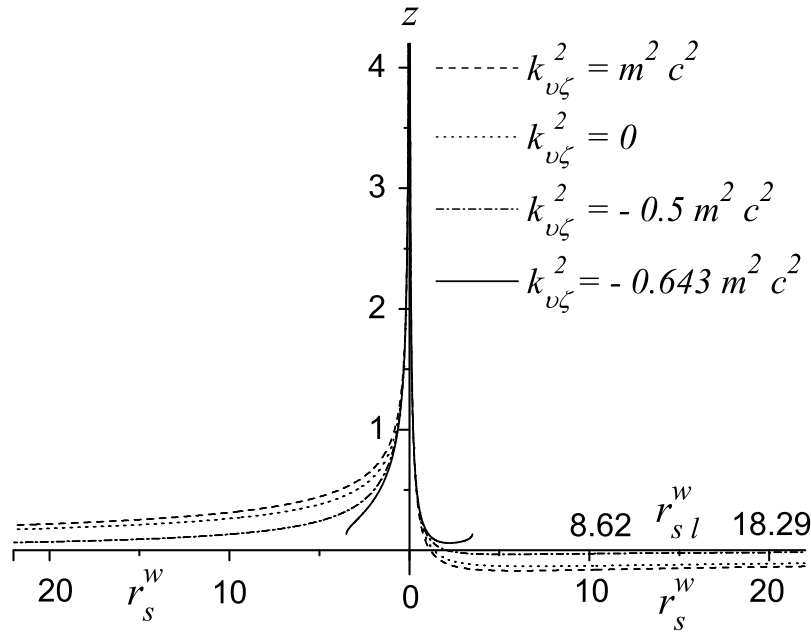


Figure 8. The combined effect of the gravitational and Doppler redshifts (see Eq.(90)). For simplicity's sake we consider the limiting case when the observer is situated at infinity. Thus, the curves on the right-hand side of the picture correspond to the sources for which $\Phi = \pi/2$, moving towards the observer, whereas the curves on the left-hand side correspond to the sources for which $\Phi = 3/2\pi$, running away from the observer.

For small enough values of r_s , the combined Doppler and gravitational effect (90) has a positive value of the redshift z for all values of $k_{\nu\zeta}^2$. Yet, for sufficiently small values of $k_{\nu\zeta}^2 < -\frac{1}{2} m^2 c^2$, e.g. for $k_{\nu\zeta}^2 = -0.643 m^2 c^2$, even the whole Doppler blueshift can be hidden behind the gravitational redshift. The breaks of the curves (with solid lines) for $k_{\nu\zeta}^2 = -0.643 m^2 c^2$ are at $r_s^{max,w} \approx 3.5$, as for $r_s^w > r_s^{max,w}$ there are no stable orbits (see Eqs.(80)-(81)).

unless the symmetry (1)-(3) is broken, the classical picture of the world follows the same patterns from the micro- to the macro-scale only if the complete integral of the system $S(t^w, r^w; d^w, l^w)$ does not change.

Transformation (93) is the symmetry of the action (1)-(3). This is the invariance of the coupled Einstein (4) and Klein-Gordon (6) equations, but it is not the invariance of their solution given by Eqs.(23) and (28). This conclusion can also be drawn from Eq.(25). Hence, we notice that the massless dilatonic field φ is the Goldstone field [56]. It would seem that invariance (93) inevitably leads to the invariance given by Eqs.(93)-(94) of the Hamilton-Jacobi equation (91). Yet, the inclusion of any term with mass $m \neq 0$ into the model given by Eq.(1) will inevitably lead to the gravitational coupling of this mass with the metric tensor part of the Lagrangian, causing the breaking of the original invariance (93). Hence, the conclusion emerges that there appears a relation between the four-dimensional mass m_4 of the particle and the parameter A [24]. This results from the Einstein equations which fix the value of A after the self-consistent inclusion of the particle with mass m into the configuration of fields. This means that the symmetry connected with the scaling (93) of A is broken.

6. Conclusions and perspectives

In this paper the non-trivial, one parametric six-dimensional “background” solution given by Eqs.(28) and (23) with the spherical symmetry in the Minkowski directions of coupled Einstein and Klein-Gordon equations has been presented [23, 22]. It consists in adding to the six dimensional gravity a massless dilatonic field, whose variation in the radial direction compensates self-consistently for the curvature. As a self-consistent [43] and non-iterative one, the solution is also non-perturbative. Here, the dilatonic “basic” field φ forms a kind of the ground field and the gravitational field (metric tensor) g_{MN} is the self-field [22, 52, 42, 43]. The gravitational component in the four-dimensional space-time is asymptotically flat but fundamentally different from the Schwarzschild solution. Locally, the space-time has the topology of the Minkowski $(1,3) \times 2$ -dimensional internal space of the varying size, i.e. the six-dimensional world is compactified in a non-homogeneous manner. Next, the motion of a test particle in the six-dimensional space-time of the obtained gravito-dilatonic Kaluza-Klein type model was examined. Additionally, in Section 4.1.1 (see Eq.(82)) it was pointed out that on the stability boundary, the relative internal angular momentum of the particle takes, beginning with zero, all consecutive values with the one half step, i.e. $\frac{M_c}{m c d} = j$, where $j = 0, \frac{1}{2}, 1, \frac{3}{2}, 2, \dots$.

In Section 2.1 both the problem of the stability of the background solution and the spectrum of the Kaluza-Klein type excitations were discussed but additional analysis of the problem can be found in [24], where the Fisher-statistical reason for six-dimensionality of the space-time was also discussed. Nevertheless, since to date we do not see any well-established experimental evidence of the multi-dimensionality of the world [26], hence, from the point of view of practical purposes, the four-dimensional consistency alone, which is possessed by a multi-dimensional model, cannot be perceived as a very

important reason for its acceptance.

Therefore, the main physical applicability of the background solution (28),(23) presented in Section 3 refers to its astrophysical and cosmological signatures for some relatively tight systems. Thus, the motion of a test particle in this background configuration was analyzed. The background solution is parameterized by the parameter A , which (especially for $r \gg A$) has similar dynamical consequences as the mass $M = A c^2 / (2 G)$ (see Note below Eq.(37)). The significance of higher terms in the metric tensor g_{MN} expansion can be different than in e.g. the Schwarzschild solution case (see e.g. Appendix B on the pericenter shift). Hence, the existence of the self-consistent gravito-dilatonic configuration (23),(28), which is perceived by an observer in the same way as invisible matter, requires taking into account the nonstandard definition of the system as one which is both under the self-consistent (Eqs.(6),(4)) and non-self-consistent (Eq.(42)) influence of the gravitational interaction. It was performed both on the astrophysical (see Section 4) and on the physics of one particle [24] levels.

As the central object does not possess a horizon (as the black-hole does), which is the frequent characteristic of more than four-dimensional solutions [20], thus one of the conclusions from the analysis of this paper is that the visible total redshift-blueshift asymmetry of the radiation from e.g. flows of sources of matter (which consist of test particles) is possible only if they are located sufficiently close to the center of the dilatonic field φ (Section 4.3). Therefore, the radiation from rotating matter, e.g. around a galaxy center, can originate from an area smaller than that connected with the corresponding Schwarzschild radius $(2 G/c^2)M$ (see Note below Eq.(37)) of a black hole. Yet, the observations of predominantly redshifted flows in the presented model can be (see Section 4) explained with special effectiveness for the motion along circular orbits with the internal momentum squared, which fulfills the relation $k_{\theta\zeta}^2 < -m^2 c^2/2$. That is, in this case in the model even the whole Doppler effect connected with the blue wing moving towards us can be hidden below the gravitational redshift effect (see Figures 7,8). Thus, real flows of the matter of some objects can be directed towards us. In fact, all galaxy- and quasar-like objects have to possess proper $k_{\theta\zeta}^2$ and four-dimensional square masses (49) in order for them to be observed as redshifted only.

Looking from the above-mentioned perspectives, two classes of phenomena are invoked below.

Firstly, the statistical analysis performed for the X-ray spectroscopy points to a need for the relativistic effects to be included when modeling the emission from the rotating matter around the galactic centers [57]. The analysis for the nucleus of the Seyfert galaxy MCG-06-30-15 [58] was followed by the one for the nuclei of the galaxies MCG-6-30-15, NGC 4593, 3C 120, MCG6-30-15, MCG5-23-16, NGC 2992, NGC 4051, NGC 3783, Fairall 9, Ark 120 and 3C 273 [57]. The conclusion was that the relativistic effects, such as the central object spin and the relativistic velocities of flows, seem to become important in shaping the overall emission line profile from the inner part of the rotating matter of accretion disks, i.e. from radii which are probably smaller than $\sim 20 A$. The characteristics of the observed emission lines can correspond to a velocity of $\sim 10^5$ km/s

which, in agreement with the analysis in Section 4.1, corresponds to a few values of A (see Figure 3). The observed lines are asymmetric, i.e. strong redshifted emission lines were detected and weaker (or none) blue-shifted ones were seen [59].

Secondly, there are also other phenomena which call for explanations and are hard to understand from the point of view of the standard lore. One class of such problems is connected with the nature of the redshift of galaxies and quasars. It has been known for a long time that the visible associations of quasars and galaxies have been observed where the components have widely discrepant redshifts [60]. We can think of a simple explanation for such seemingly strange phenomena in terms of the presented model. That is, let us imagine that a quasar–galaxy system is captured by the gravito-dilatonic configuration of the field φ (see 6th row in Table 1). Supposing that both the quasar and galaxy are moving along stable orbits, we apply the results obtained in Section 4. If the things are so arranged that the quasar (or a group of them) is closer to the center of the background gravito-dilatonic field configuration, then it has a redshift greater than the galaxy located peripherally. As has been illustrated in Figures 7,8, the smaller the radius r_s^w of the stable orbit of the quasar is the more significant this effect also is.

Remark: *Nevertheless, quasar-like objects are also seen in the vicinity of the central parts of some galaxies. This could be a sign that a galaxy nucleus consists of the background gravito-dilatonic field configuration (see 3rd row in Table 1). The visibility of bigger values of the redshift of the luminous matter from the inner part of this galaxy nucleus could be blocked by the clumping of the matter orbiting and infalling on it.*

Recently a large quasar group (LQG) with 73 members with a huge redshift range $1.1742 \leq z \leq 1.3713$ was identified in the DR7QSO catalogue of the Sloan Digital Sky Survey [61]. Such a spread of quasars' redshift can be understood as resulting from bounding them in one node of the gravito-dilatonic configuration.

Note: The four-dimensional part of the metric tensor (9) possesses a spherical symmetry. Thus, it should be emphasized that in reality the orbits do not necessarily lay on one plane. Next, the instantaneous position of an object in space is observed as projected onto a two-dimensional sphere along the light's geodesics in the curved space-time. This sphere is then seen as a plane perpendicular to us only. This can obviously place some objects with bigger r_s seemingly closer to the center of the background gravito-dilatonic field configuration. Finally, if constant \mathcal{C} in Eq.(78) does not have the same value for all orbiting objects then their proper tangent velocities, (77), depend on \mathcal{C} and the observational situation gets more complex.

When the distance from the center is a fraction of A , the combined gravitational and Doppler redshift given by Eq.(90) becomes the sloping function of r_s^w thus disclosing the existence of a big redshift discrepancy. Such a possibility also has an attractive feature that if the quasar–galaxy constitutes a kind of binary system, then the visible bridge of matter connecting the galaxy and quasar may be explained as a sign of an infall (from the galaxy to the center of the field φ) of matter that is passing through the quasar.

Let us also recall that near the center of the field φ the space-time curvature (25) is large, strongly accelerating (see Eq.(85)) the infalling particles. Therefore, even if the diameter of the quasar size is of ~ 100 AU only then due to the fact that the quasar is located near the center of φ , does the existence of the highly nonuniform and anisotropic gravitational field across the quasar interior cause the appearance of large tidal forces inside it. This sheds some light on the nature of the quasar emission as connected with the ultrahigh relative acceleration of particles in its interior, also charged ones, which are mainly electrons. The idea briefly outlined above deserves further, deeper considerations.

Meanwhile, if a galaxy was close to the center of the field φ , let's say in a stable orbit with $r_s \sim A/2$ (see Figure 4,5), then due to its size it would have been torn into pieces by the tidal forces of the gravito-dilatonic center. This means that the only possibility for a “galaxy” to possess a bigger redshift is to be placed at the center of the background gravito-dilatonic field configuration with the central, highly redshifted opaque inner part of this “galaxy” being severely overshadowed by the more peripheral luminous matter. This overshadowing could account for its faintness. However, this means that e.g. an object like UDFj-39546284 [62] is not really a “usual” galaxy. Nevertheless, the real obstacle in the precise identification of these objects is the lack of their observed detailed structure. With the lack of the confirmation that objects like these emit all wavelengths both shorter than $1.34 \mu\text{m}$ and longer than $1.6 \mu\text{m}$, the spectroscopy analysis [62, 63] increases the doubt about their true galaxy structure .

What is more, there is a great deal of evidence that redshift is at least partially the intrinsic property of galaxies and quasars that is apparently quantized [64, 65, 66, 67, 68]. Its nature is not yet understood and an analysis of this phenomenon is not covered by the presented, classical model. The solution to the problem may require e.g. the modification of the background metric so that the modified one possesses additional minima in the component g_{rr} . This could be achieved by coupling the Einstein equations (4) to the one which replaces the Klein-Gordon equation (6) and only then solving the Hamilton-Jacobi equation used in this paper for the description of the motion of test particles. The other possibility for obtaining additional minima of the effective potential \mathcal{U}_{eff} could be realized by introducing a new wave function $\Psi(x^M) = \mathcal{R}(x^M) \exp(i S(x^M))$ for a “quasar” system, which fulfills the Klein-Gordon equation (similarly as in [24]), where $\mathcal{R}(x^M)$ and $S(x^M)$ are two real field functions. Thus $S(x^M)$ fulfills the equation which is formally similar to the Hamilton-Jacobi one, (42), except for the modification of the effective potential caused by a potential of the Bohm's type (compare [69, 70]). (As Bohm argued, $S(x^M)$ is in this case a general integral and not the complete one.)

Remark: *The self-consistent gravitational coupling of the matter field $\Psi(x^M)$ (included into the total fields configuration) with the metric tensor causes the breaking of the scale invariance of the action (1)-(3), connected with scaling of A (see Section 5). Thus, due to the Einstein equations, a relation between the four-dimensional mass m_4 and the parameter A appears whose value is fixed in this way (compare [24]).*

An analysis of these two possibilities will be presented in following papers.

Next, it would be of observational importance to examine e.g. the apparent surface brightness \mathcal{A} of such sources as galaxies. Let d_L be the (bolometric) luminosity distance and d_A the angular size distance of a galaxy. Then \mathcal{A} is the quotient of the total flux received by the observer, which behaves like d_L^{-2} , to the angular area of the galaxy that is seen by the observer, which goes as d_A^{-2} , i.e. $\mathcal{A} \propto (d_A/d_L)^2$. Thus, it would be easy to notice that \mathcal{A} is the function of both the (combined) redshift z , (90), and the real distance R from the source to the observer.

Remark: *Because of the integral form (37) of the physical radial distance of the source from the center of the background gravito-dilatonic field configuration, the apparent surface brightness \mathcal{A} cannot be written as a simple analytical expression.*

Simultaneously, it would also be of interest to examine interactions of the dilatonic-like centers and their distribution $\rho(\varphi)$ in the universe in order to understand its state. The analysis of \mathcal{A} as the function of z and R , which depends on $\rho(\varphi)$, will be discussed in following papers.

Finally, the observations mentioned above [71] are still growing in number [72]. These and others [61], like e.g. the helium abundance in the blue hook stars [73], have no reasonable explanation within the standard interpretation that claims e.g. that the Hubble expansion is responsible for the redshifts of galaxies or within the theories with the continuous self-creation of matter and the variable mass hypothesis.

There is certainly a need for new models; however, seeking them among the evolutionary ones is not the proper way.

Acknowledgments

This work has been supported by L.J.Ch..

Thanks to Marek Biesiada for the discussions. This work has been also supported by the Department of Field Theory and Particle Physics, Institute of Physics, University of Silesia.

Appendix A. The solution for $A < 0$

If the parameter $A < 0$, then Eqs.(21)-(23) are valid only when $r > |A|$. Likewise, in Section 3 we write the temporal and radial components of the metric g_{MN} and the internal “radius” $\varrho(r)$ (see Eqs.(22) and (28))

$$\begin{cases} g_{tt} = \frac{r}{r-|A|} \\ g_{rr} = -\frac{r}{r-|A|} \\ \varrho(r) = d_{out} \sqrt{\frac{r-|A|}{r}} \end{cases} \quad (\text{A.1})$$

As in Section 2, we have $g_{tt} \rightarrow 1$ for $r \rightarrow \infty$ (see Eq.(36)). But, comparing the gravitational potential $g_{tt} = \frac{r}{r-|A|} \approx 1 + \frac{|A|}{r}$ for $r \gg |A|$ with $g_{tt} = 1 - \frac{G}{c^2} \frac{M}{r}$, which is the one induced by a mass M in the Newtonian limit, we notice that the gravitational potential g_{tt} (see Eq.(A.1)) is a repulsive one, contrary to the case for $A > 0$.

The formulae for the scalar curvature \mathcal{R} (see Eq.(25)) and dilatonic field φ Eq.(23) now have the form

$$\mathcal{R} = \frac{A^2}{2r^3(r-|A|)} \quad (\text{A.2})$$

$$\varphi(r) = \pm \sqrt{\frac{1}{2\kappa_6}} \ln\left(\frac{r}{r-|A|}\right), \quad (\text{A.3})$$

where d_{out} is the constant.

From (A.1) we see that the metric tensor becomes singular at $r = |A|$. However, its determinant g (see Eq.(29)) remains well defined. Nevertheless, we notice that because at $r = |A|$ the curvature scalar \mathcal{R} becomes singular and for $r \leq |A|$ the field φ is not defined, hence this metric singularity is a genuine one and a system is well posed only for $r > |A|$.

Thus, from Eqs.(A.2)-(A.3), it follows that the physical radial distance can be calculated outside the surface $r = |A|$ only and its value, e.g. from the radius $|A|$ to the radius $r > |A|$, is equal to

$$\begin{aligned} r_{l-A} &= \int_{|A|}^r dr \sqrt{-g_{rr}} \\ &= \sqrt{\frac{r}{r-|A|}} (r-|A|) + \frac{1}{2} |A| \ln \left(\frac{-|A| + 2r + 2(r-|A|) \sqrt{\frac{r}{r-|A|}}}{|A|} \right) > r-|A|. \end{aligned} \quad (\text{A.4})$$

The region $r > |A|$ is the only one where a frequency shift can be observed. Using Eq.(A.1) we can rewrite Eq.(39) as follows

$$\frac{\omega_{obs}}{\omega_\sigma} = \frac{\sqrt{\frac{r_\sigma}{r_\sigma-|A|}}}{\sqrt{\frac{r_{obs}}{r_{obs}-|A|}}} \quad (\text{A.5})$$

Like before, we take for simplicity's sake the limit when the observer is in infinity. So we get (see Figure A1)

$$\frac{\omega_{obs}}{\omega_\sigma} = \sqrt{\frac{r_\sigma^w}{r_\sigma^w - 1}}, \quad \text{where } r_\sigma^w = \frac{r_\sigma}{|A|} \text{ and } r_\sigma > |A|. \quad (\text{A.6})$$

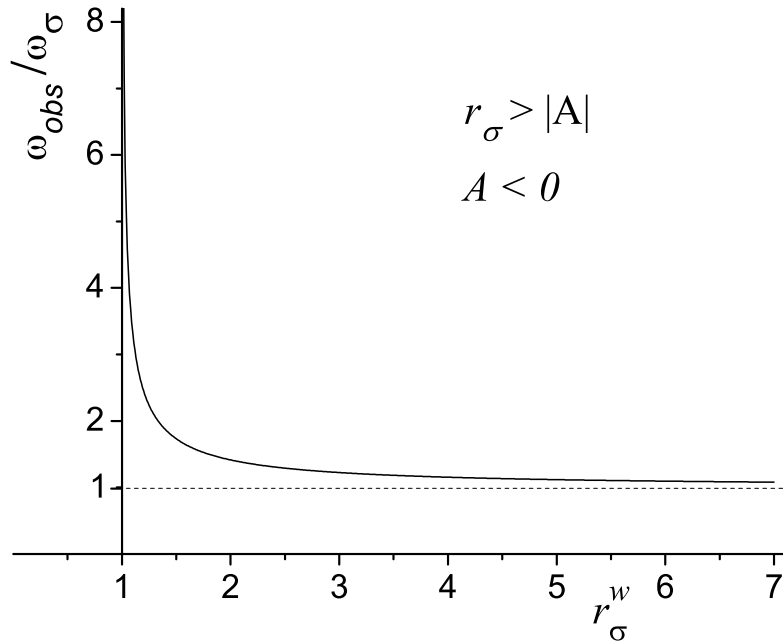


Figure A1. The ratio of the frequency ω_{obs} of the photon which reaches the observer (which is at infinity) to the frequency ω_σ of the photon emitted from the source at $r_\sigma > |A|$ ($A < 0$) as a function of the relative radius $r_\sigma^w = \frac{r_\sigma}{|A|}$.

We obtained the result that the nearer the source was to the surface given by the equation $r = |A|$ the more the emitted photon which reaches the observer would be blueshifted. This property, caused (in this case) by the repulsive character of the gravitational potential, is the reason why this solution was omitted in the main text, as to date it is rather unnoticed in observations. But, because it formally provides a solution to the model, some of its properties have been reproduced here.

Appendix B. Pericenter shift

Let us consider the shift of the point with the minimal r_s , which is the pericenter for a test particle elliptically orbiting a central mass M in the spherically symmetric time-independent metric. In Section 3 we pointed out that in the expansion of the metric to the first order in $\frac{A}{r}$, the parameter $A/2$ has similar dynamical consequences as the mass M . The approximate post-Newtonian expression for g_{tt} and g_{rr} of the general metric

generated by a central mass M can be written as follows [74]

$$\begin{aligned} g_{tt} &\cong \left(1 - \frac{2M}{r} + 2(\beta - \gamma)\frac{M^2}{r^2}\right) \\ g_{rr} &\cong -\left(1 + 2\gamma\frac{M}{r}\right). \end{aligned} \quad (\text{B.1})$$

At the lowest order of $\frac{M}{r}$ beyond the Newtonian theory, an orbit undergoes a pericenter shift [74, 75] given by

$$\Delta\Phi = \frac{6\pi M}{a(1-e^2)} \times \frac{(2+2\gamma-\beta)}{3}, \quad (\text{B.2})$$

where a is the semi-major axis of the Newtonian ellipse and e is the eccentricity ($e < 1$ for an ellipse and $e = 0$ for the circle).

The expression (B.2) is useful for testing different metric theories of gravity with different field equations. For example if we substitute $\gamma \equiv \beta = 1$, corresponding to the general relativity, we get

$$\Delta\Phi = \frac{6\pi M}{a(1-e^2)}. \quad (\text{B.3})$$

Now, let us use the formula given by Eq.(B.2) for the pericenter shift of a test particle orbiting the center of the dilatonic field φ , (23), with the metric tensor given by Eq.(28) coupled to this field. Neglecting the influence of the internal two-dimensional space (which is reasonable for $r \gg A$) and expanding g_{tt} and g_{rr} given by Eq.(28) to the second and first order in $\frac{A}{r}$, respectively, we obtain

$$g_{tt} \approx 1 - \frac{A}{r} + \frac{A^2}{r^2} \quad \text{and} \quad g_{rr} \approx -\left(1 - \frac{A}{r}\right). \quad (\text{B.4})$$

Comparing (B.4) with the approximate post-Newtonian result (B.1), for $M := A/2$ we get the following approximate values of the post-Newtonian parameters in our model

$$\gamma = -1 \quad \text{and} \quad \beta = 1, \quad \text{for } r \gg A. \quad (\text{B.5})$$

Hence, from Eq.(B.2) we finally obtain

$$\Delta\Phi = -\frac{\pi A}{a(1-e^2)}. \quad (\text{B.6})$$

Thus, e.g. for a test particle on the orbit with the radius $r_s = a$, where $a/A = 100$ (see Table 1 for values of A), the pericenter shift is equal to $(-1^\circ 48' / \text{revolution})$ and $(-9^\circ 28' / \text{revolution})$ for $e = 0$ and $e = 0.9$, respectively. In the post-Newtonian approximation used, the negative sign is characteristic for the influence of the dilatonic field which leads to a retrograde pericenter shift.

References

- [1] C.W.F. Everitt et al., *Gravity Probe B: Final Results of a Space Experiment to Test General Relativity*, Phys.Rev.Lett. **106**, 221101, doi:10.1103/PhysRevLett.106.221101, (2011). J. Beringer et al.(PDG), Chapter 20 on *Experimental tests of gravitational theory*, T. Damour, (October 2011), PR D **86**, 010001, (2012), <http://pdg.lbl.gov>.
- [2] { *The analysis could be performed in accordance with an effective gravity theory of the Logunov type [3] with, of course, somehow different consequences.* }
- [3] V.I. Denisov and A.A. Logunov, *The Theory of Space-Time and Gravitation*, in *Gravitation and Elementary Particle Physics*, Physics Series, ed. A.A. Logunov, (MIR Publishers, Moscow), 14-130, (1983). C. Lämmerzahl, *Testing Basic Laws of Gravitation Are Our Postulates on Dynamics and Gravitation Supported by Experimental Evidence?* in *Mass and Motion in General Relativity*, Editors: L. Blanchet, A. Spallicci, B. Whiting, (Springer), 25-65, (2011). G. F. R. Ellis, *Note on Varying Speed of Light Cosmologies*, *General Relativity and Gravitation* **39** (4), 511520, (2007), arXiv:astro-ph/0703751v1.
- [4] I. Bars, J. Terning, F. Nekoogar (Founding Ed.), *Extra Dimensions in Space and Time*, (Springer), (2010). J. Beringer et al., (Particle Data Group), J. Parsons, A. Pomarol, Chapter on *Extra Dimensions*, 4-5, (November 2011), PR D **86**, 010001, URL:<http://pdg.lbl.gov>, (2012).
- [5] M.B. Green and J.H. Schwarz, *Supersymmetrical dual string theory*, Nucl. Phys. B **181**, 502-530, (1981). M.B. Green and J.H. Schwarz, *Supersymmetric dual string theory III*, Nucl.Phys.B **198**, 441, (1982). M. Kaku, *Introduction to Superstrings*, (Springer, New York), (1988).
- [6] R. Kerner, *Generalization of the Kaluza-Klein theory for an arbitrary non-abelian gauge group*, Ann.Inst. H. Poincaré, Vol.**IX**, no.2, 143-152, (1968).
- [7] D. Bailin, A. Love, *Kaluza-Klein theories*, Rep.Prog.Phys. **50**, 1087-1170, (1987).
- [8] Y. Choquet-Bruhat, *General Relativity and Einsteins Equations*, pp.653-662,742, (Oxford Univ. Press), (2009).
- [9] M.B. Green, J.H. Schwarz, E. Witten, *Superstring theory, Vol.2, Loop amplitudes, anomalies & phenomenology*, (Cambridge Univ. Press), (1988). W.-Z. Feng, D. Lüst, O. Schlotterer, Nucl.Phys. B **861**, 175-235, doi:10.1016/j.nuclphysb.2012.03.010, (2012).
- [10] The BABAR Collaboration, *Evidence for an excess of $\bar{B} \rightarrow D^* \tau^- \bar{\nu}_\tau$ decays*, SLAC-PUB-15028, arXiv:1205.5442v1, 24 May 2012.
- [11] J.Y. Bang, M.S. Berger, *Quantum mechanics and the generalized uncertainty principle*, Phys.Rev.D **74**, pp.125012:1-8, doi:10.1103/PhysRevD.74.125012, (2006). Ben-Rong Mu, Hou-Wen Wu, Hai-Tang Yang, *Generalized Uncertainty Principle in the Presence of Extra Dimensions*, Chin.Phys.Lett. Vol.**28**(9), 091101, doi:10.1088/0256-307X/28/9/091101, (2011).
- [12] M. Ozawa, Universal Uncertainty Principle, Simultaneous Measurability, and Weak Values, (QCMC): The Tenth International Conference 2010, AIP Conf. Proc. **1363**, 53-62, doi:<http://dx.doi.org/10.1063/1.3630147>, (2011), arXiv:1106.5083v2.
- [13] *The nature of light. What is a photon?*, pp.372,374, Edited by Ch. Roychoudhuri, A.F. Kracklauer, K. Creath, (CRC Press, Taylor&Francis Group), (2008).
- [14] J. Śladkowski, J. Syska, *Information channel capacity in the field theory estimation*, Phys.Lett.A **377** 18-26, doi:10.1016/j.physleta.2012.11.002, (2012), arXiv:1212.6105.
- [15] J. Erhart, S. Sponar, G. Sulyok, G. Badurek, M. Ozawa and Y. Hasegawa, *Experimental demonstration of a universally valid error/disturbance uncertainty relation in spin measurements*, Nature Physics **8**, 185189, doi:10.1038/nphys2194, (2012).
- [16] C. Roychoudhuri, *Foundations of Physics* 8 (11/12), 845 (1978). J. Syska, *Has Quantum Field Theory the Standard Transition from Poisson Brackets?*, Int.J. of Theoretical Phys., Vol.**42**, No.5, 1085-1088, (2003).
- [17] M. Spanner, I. Franco and P. Brumer, *Coherent control in the classical limit: Symmetry breaking in*

- an optical lattice, Phys.Rev.A **80**, 053402, doi:10.1103/PhysRevA.80.053402, (2009). A. Matzkin, *Entanglement in the classical limit: Quantum correlations from classical probabilities*, Phys.Rev.A **84**, 022111, doi:10.1103/PhysRevA.84.022111, (2011).
- [18] {As a consequence the UR loses its contact with the observational results and has to be abandoned on behalf of the multiparametric Rao-Cramér inequality, as not only the operational but the more fundamental one [19, 14].}
- [19] J. Syska, *Maximum likelihood method and Fisher's information in physics and econophysics, (polish version)*, University of Silesia, arXiv:1211.3674 [physics.gen-ph], <http://el.us.edu.pl/ekonofizyka/images/f/f2/Fisher.pdf>, (2011).
- [20] P.S. Wesson, *A physical interpretation of Kaluza-Klein cosmology*, Ap.J **394**, 19, (1992). P. Lim, J.M. Overduin and P.S. Wesson, J. Math. Phys. **36**, 6907, (1995). D. Kalligas, P.S. Wesson, and C. W. F. Everitt, *The Classical tests in Kaluza-Klein gravity*, Ap.J, Part 1, vol. **439**, no.2, 548557, (1994).
- [21] R. Mańka and J. Syska, *Torus compactification of six-dimensional gauge theory*, J.Phys.G: Nucl.Part.Phys. **15**, 751-764, (1989).
J. Syska, *Remarks on self-consistent models of a particle*, Trends in Boson Research, e.d. A.V. Ling, (Nova Science Publishers), 163-181, (2006).
- [22] J. Syska, *Self-consistent classical fields in field theories*, PhD thesis (unpublished), (University of Silesia), (1995/99).
- [23] M. Biesiada, R. Mańka and J. Syska, *A new static spherically symmetric solution in six-dimensional dilatonic Kaluza-Klein theory*, Inter.Journal of Modern Physics **D**, Vol.**9**, Nu.1, 71-78, (2000); R. Mańka and J. Syska, *Nonhomogeneous six-dimensional Kaluza-Klein compactification*, preprint UŚL-TP-95/03, (University of Silesia), (1995).
- [24] J. Syska, *Kaluza-Klein Type Model for the Structure of the Neutral Particle-like Solutions*, Int.J.Theor.Phys., Vol.**49**, Issue 9, 2131-2157, doi:10.1007/s10773-010-0400-8, Open Access, (2010).
- [25] G. Bertone, G. Servant and G. Sigl, *Indirect detection of Kaluza-Klein dark matter*, Phys.Rev. D **68**, 044008, (2003). A.F. Zakharov, F. De Paolis, G. Ingrosso, A.A. Nucita, *Shadows as a tool to evaluate black hole parameters and a dimension of spacetime*, New Astronomy Reviews, Vol.**56**, Issues 23, 6473, (2012).
- [26] S. Chatrchyan et al. (CMS Collaboration), *Search for Signatures of Extra Dimensions in the Diphoton Mass Spectrum at the Large Hadron Collider*, PRL **108**, 111801, (2012).
- [27] J.H. Oort, *The force exerted by the stellar system in the direction perpendicular to the galactic plane and some related problems*, Bull.Astr.Inst. Netherlands **VI**, 249-287, (1932).
- [28] F. Zwicky, *Die Rotverschiebung von extragalaktischen Nebeln*, Helv.Phys.Acta **6**, 110-127, (1933).
- [29] E. Öpik, Bull. de la Soc. Astr. de Russie **21**, 150,(1915).
- [30] V.C. Rubin and W.K. Ford, Ap.J **379**, (1970). V.C. Rubin, W.K. Ford, and N. Thonnard, *Rotational Properties of 21 Sc galaxies with a large range of luminosities and radii. From NGC 4605 (R = 4 kpc) to UGC 2885 (R = 122 kpc)*, Ap.J **238**, 471, (1980).
- [31] E.I. Gates, G. Gyuk, and M.S. Turner, *Microlensing and Halo Cold Dark Matter*, Phys.Rev.Lett. **74**, 3724-3727, (1995). E.I. Gates, G. Gyuk and M.S. Turner, *The Local Halo Density*, Ap.J.Lett., **449**, L123L126, (1995).
- [32] P. Tisserand et al., *Limits on the Macho content of the Galactic Halo from the EROS-2 Survey of the Magellanic Clouds*, 387-404, A&A **469**, doi: 10.1051/0004-6361:20066017, (2007). L. Wyrzykowski, J. Skowron, S. Kozłowski, A. Udalski, M.K. Szymański, M. Kubiak, G. Pietrzyński, I. Soszyński, O. Szewczyk, K. Ulaczyk, R. Poleski and P. Tisserand, *The OGLE view of microlensing towards the Magellanic Clouds IV. OGLE-III SMC data and final conclusions on MACHOs*, Mon.Not.R.Astron.Soc., **416**, 29492961, doi: 10.1111/j.1365-2966.2011.19243.x, (2011). S. Calchi Novati, *Microlensing towards the Magellanic Clouds and M31: is the quest for MACHOs still open?*, J.Phys.: Conf.Ser. **354**, 012001, doi:10.1088/1742-6596/354/1/012001, (2012).

- [33] The Review of Particle Physics, K. Nakamura et al. (Particle Data Group), Chapter **22**, 1-19, *Dark matter*, Revised September 2011 by M. Drees (Bonn University) and G. Gerbier (Saclay, CEA), J.Phys.G **37**, 075021 (2010) and 2011 partial update for the 2012 edition. M.J. Disney, J.D. Romano, D.A. GarciaAppadoo, A.A. West, J.J. Dalcanton and L. Cortese, *Galaxies appear simpler than expected*, Nature **455**, 1082-1084, doi:10.1038/nature07366, (23 October 2008). R.H. Sanders, *Modified Newtonian Dynamics: A Falsification of Cold Dark Matter*, Advances in Astronomy, Volume 2009, (2009), Article ID 752439, doi:10.1155/2009/752439. P. Kroupa, *The dark matter crisis: falsification of the current standard model of cosmology*, (2012), arXiv:1204.2546v1. P. Kroupa, B. Famaey, K.S. de Boer, J. Dabringhausen, M.S. Pawlowski, C.M. Boily, H. Jerjen, D. Forbes, G. Hensler, and M. Metz, *Local-Group tests of dark-matter concordance cosmology. Towards a new paradigm for structure formation*, (2010), arXiv:1006.1647v3.
- [34] { *This dilatonic field φ is the created fluctuation out from nothingness (my footnote).* }
 P. Forgács, J. Gyürüsi, *Static spherically symmetric monopole solutions in the presence of a dilaton field*, Phys.Lett.B **366**, pp.205-211, doi:10.1016/0370-2693(95)01321-0, (1996), arXiv:hep-th/9508114v2.
 G. Chechelashvili, G. Jorjadze, *Dilaton Field and Massless Particle for 2d Gravity*, Workshop ISPM-98, Tbilisi September 12-18, (1999), arXiv:hep-th/9908206.
- [35] M. Biesiada, K. Rudnicki and J. Syska, *An alternative picture of the structure of galaxies*, in *Gravitation, Electromagnetism and Cosmology: toward a new synthesis*, ed. K. Rudnicki, (Apeiron, Montreal), 31-47, (2001).
- [36] M. Nishino and E. Sezgin, *Matter and gauge couplings of $N = 2$ supergravity in six dimensions*, Phys. Lett. **B 144**, 187-192, (1984). E. Bergshoeff, A. Salam and E. Sezgin, *A supersymmetric R^2 -action in six dimensions and torsion*, Phys.Lett.B **173**, 73-76, (1986). A. Salam and E. Sezgin, *Chiral compactification on Minkowski $\times S^2$ of $N=2$ Einstein-Maxwell supergravity in six dimensions*, Phys.Lett. **B 147**, 47, (1984).
- [37] V.D. Ivashchuk and V.N. Melnikov, Class.Quantum Grav. **11**, 1793, (1994). V.D. Ivashchuk and V.N. Melnikov, Grav. & Cosmol. **1** No2, 133, (1995); V.D. Ivashchuk, PhD Dissertation, (VNICPV, Moscow), (1989).
- [38] K.A. Bronnikov and V.N. Melnikov, Annals of Physics (N.Y.) **239**, 40, (1995).
- [39] { *The dimension of the resulting space-time for the multi-dimensional field theory model depends on the number \aleph of degrees of freedom of the field in our four-dimensional Minkowski space-time [24, 44]. For example, in the case of electromagnetism for which $\aleph = 4$, the arising space-time is eight-dimensional. The obtained field theory model is called the Kaluza-Klein type model.* }
- [40] G.I. Barenblatt, *Scaling*, (Cambridge Univ. Press), (2003).
- [41] { *Thanks to Ryszard Mańka for pointing in this direction.* }
- [42] J. Syska, *Boson ground state fields in the classical counterpart of the electroweak theory with non-zero charge densities*, in *Frontiers in field theory*, ed. O. Kovras, (Nova Science Publishers), (New York 2005), chapter 6, 125-154 and in *Focus on Boson Research*, (Nova Publishers), 233-258, (2006), arXiv:hep-ph/0205313.
- [43] J. Syska, *The weak bound state with the non-zero weak charge density as the LHC 126.5 GeV state*, paper in the review, (2013), arXiv:1305.1237 [hep-ph].
- [44] B.R. Frieden, *A probability law for the fundamental constants*, Found.Phys., Vol.**16**, No.9, 883-903, (1986). B.R. Frieden, *Fisher information, disorder, and the equilibrium distributions of physics*, Phys.Rev.A **41**, 4265-4276, (1990). B.R. Frieden, B.H. Soffer, *Lagrangians of physics and the game of Fisher-information transfer*, Phys.Rev.E **52**, 2274-2286, (1995). B.R. Frieden, *Relations between parameters of a decoherent system and Fisher information*, Phys.Rev.A **66**, 022107, (2002). B.R. Frieden, A. Plastino, A.R. Plastino and B.H. Soffer, *Schrödinger link between nonequilibrium thermodynamics and Fisher information*, Phys.Rev.E **66**, 046128, (2002). B.R. Frieden, A. Plastino, A.R. Plastino and B.H. Soffer, *Non-equilibrium thermodynamics and Fisher information: An illustrative example*, Phys.Lett.A **304**, 73-78, (2002). B.R. Frieden, Science

- from Fisher information: A unification, (Cambridge Univ. Press), (2004).
- [45] J. Syska, *Fisher information and quantum-classical field theory: classical statistics similarity*, Phys. Stat. Sol.(b) **244**, No.7, 2531-2537, (2007)/DOI 10.1002/pssb.200674646, arXiv:physics/0811.3600.
- E.W. Piotrowski, J. Śladkowski, J. Syska, S. Zajac, *The method of the likelihood and the Fisher information in the construction of physical models*, Phys. Stat. Sol.(b), **246**, No.5, 1033-1037, (2009)/DOI 10.1002/pssb.200881566, arXiv:physics/0811.3554.
- [46] J. Syska, *Frieden wave-function representations via an Einstein-Podolsky-Rosen-Bohm experiment*, Phys.Rev.E. **88**, No.3, 032130, doi:10.1103/PhysRevE.88.032130, (2013).
- [47] M. Peixoto, *Structural stability on two-dimensional manifolds*, Topology **1**, Issue 2, 101120, (1962). M. Brin, G. Stuck, Introduction to dynamical systems, (Cambridge Univ. Press), (2003).
- [48] A.D. Rendall, Partial differential equations in general relativity, pp.19,180-184, (Oxford Univ. Press), (2008).
- [49] {Because of this, e.g. quantum chromodynamics (QCD) is a theory without final fundamental success, as was expressed in [50]: "... all spin parts [of the nucleon] have to add to $\frac{1}{2}$ which is incredible in the light of the present day experiments. This may indicate that some underlying symmetries, unknown at present, are playing a role in forming the various contributing parts such that the final sum rule gives the fermion $\frac{1}{2}$ value". In this respect the theoretical situation of QCD (which by composing nucleon from point-like "partons" has recently proposed a kind of a "planetarian" approach) has not improved at all [51]. Its problem, contrary to the self-consistent approach [22, 52, 42, 43], consists in an attempt to regain the classical non-zero extended charge density that was quantized earlier. }
- [50] K. Heyde, *Basic ideas and concepts in nuclear physics*, 3rd ed., IOP Publishing Ltd, p.577, (2004).
- [51] F. Gross, G. Ramalho and M.T. Peña, (2012), arXiv:1201.6337v1 .
- [52] R. Mańka and J. Syska, Phys.Rev.D **49**, Nu.3, pp.1468-78, (1994). This paper is drastically reinterpreted by [42] and [43].
- [53] B.O. Barut, J. Kraus, *Nonperturbative quantum electrodynamics: The Lamb shift*, Found.Phys. **13**, 189-194, doi:10.1007/BF01889480, (1983). A.O. Barut, J.F. Van Huele, *Quantum electrodynamics based on self-energy: Lamb shift and spontaneous emission without field quantization*, Phys.Rev.A **32**, 3187-3195, doi:10.1103/PhysRevA.32.3187 , (1985). A.O. Barut, J.P. Dowling, *Quantum electrodynamics based on self-energy: Spontaneous emission in cavities*, Phys.Rev.A **36**, 649-654, doi:10.1103/PhysRevA.36.649 , (1987). A.O. Barut, *Combining relativity and quantum mechanics: Schrödinger's interpretation of ψ* , Found.Phys. **18**, 95-105, doi:10.1007/BF01882875, (1988); *Schrödinger's interpretation of psi as a continuous charge distribution*, Ann.Phys. (Leipzig), **45**, 31-36, (1988); *The revival of Schrödinger's interpretation of quantum mechanics*, Found.Phys.Lett. **1**, 47-56, doi:10.1007/BF00661316, (1988). A.O. Barut, *Quantum-electrodynamics based on self-energy*, Phys.Scr. T **21**, 18-21, (1988); A.O. Barut, Y.I. Salamin, *Relativistic theory of spontaneous emission*, Phys.Rev.A **37**, 2284-2296, doi:10.1103/PhysRevA.37.2284 (1988). A.O. Barut and N. Ünal, *An exactly soluble relativistic quantum two-fermion problem*, J.Math.Physics **27**, 3055, doi:10.1063/1.527235, (1986); A.O. Barut and N. Ünal, Physica A **142**, *A new approach to bound-state quantum electrodynamics: I. Theory*, 467-487, doi:10.1016/0378-4371(87)90036-7, and *A new approach to bound-state quantum electrodynamics: II. Spectra of positronium, muonium and hydrogen*, 488-497, doi:10.1016/0378-4371(87)90037-9, (1987).
- [54] L.D. Landau and E.M. Lifshitz, *The classical Theory of Fields*, (Pergamon Press, New York), (1975). V. Petkov, *On the gravitational redshift*, (2001), arXiv:gr-qc/9810030; *Propagation of light in non-inertial reference frames*, (2003), arXiv:gr-qc/9909081v7.
- [55] W. Rubinowicz and W. Królikowski, *Mechanika teoretyczna*, (Polish Scientific Publishers, Warszawa), (1980). E.T. Whittaker, *A Treatise on the Analytical Dynamics of Particles and Rigid Bodies*, (Cambridge Univ. Press, London), (1904).
- [56] M.B. Green, J.H. Schwarz, E. Witten, *Superstring theory*, Vol.2, chapter 13, (Cambridge Univ.

- Press), (1988).
- [57] L.W. Brenneman and Ch.S. Reynolds, *Relativistic broadening of iron emission lines in a sample of active galactic nuclei*, *Ap.J* **702**, No.2, 1367-1386, doi:10.1088/0004-637X/702/2/1367, (2009). M. Guainazzi, S. Bianchi, M. Doveiak, *Statistics of relativistically broadened Fe K α lines in AGN*, *Astron.Nachr.*, Vol.**327**, Issue 10, 1032, (2006).
- [58] L.W. Brenneman and Ch.S. Reynolds, *Constraining black hole spin via X-ray spectroscopy*, *Ap.J*, **652**, 1028-1043, (2006).
- [59] Y. Tanaka, K. Nandra, A.C. Fabian, H. Inoue, C. Otani, T. Dotani, K. Hayashida, K. Iwasawa, T. Kii, H. Kunieda, F. Makino, M. Matsuoka, *Gravitationally redshifted emission implying an accretion disk and massive black hole in the active galaxy MCG63015*, *Nature* **375**, 659-661, (1995). M. Guainazzi, et al., *A&A* **341**, L27, (1999). K. Iwasawa, et al., *MNRAS* **282**, 1038, (1996). M. Guainazzi, et al., *A&A* **341**, L27, (1999). J.C. Lee, A.C. Fabian, W.N. Brandt, C.S. Reynolds, & K. Iwasawa, *MNRAS* **310**, 973, (1999). J.C. Lee, A.C. Fabian, C.S. Reynolds, W.N. Brandt, & K. Iwasawa, *MNRAS* **318**, 857, (2000). J.C. Lee, K. Iwasawa, J.C. Houck, A.C. Fabian, H.L. Marshall, & C.R. Canizares, *ApJ* **570**, L47, (2002). A.J. Young, J.C. Lee, A.C. Fabian, C.S. Reynolds, R.R. Gibson, & C.R. Canizares, *ApJ* **631**, 733, (2005). J. Wilms, C.S. Reynolds, M.C. Begelman, J. Reeves, S. Molendi, R. Staubert, & E. Kendziorra, *MNRAS* **328**, L27, (2001). A.C. Fabian, et al., *MNRAS* **335**, L1, (2002). C.S. Reynolds, J. Wilms, M.C. Begelman, R. Staubert, & E. Kendziorra, *MNRAS* **349**, 1153, (2004).
- [60] H. Arp, E. Giraud, J.W. Sulentic and J.P. Vigier, *Pairs of spiral galaxies with magnitude differences greater than one*, *A&A* **121**, No.1, 26-28, (1983).
- [61] R.G. Clowes, K.A. Harris, S. Raghunathan, L.E. Campusano, I.K. Söchting, M.J. Graham, *A structure in the early Universe at $z \sim 1.3$ that exceeds the homogeneity scale of the R-W concordance cosmology*, *MNRAS* **429**, pp.2910-2916, doi:10.1093/mnras/sts497, (2013).
- [62] R.J. Bouwens, G.D. Illingworth and the HUDF09 Team, *Supplementary Information for Nature Letter Searches and limits for $z \sim 10$ galaxies in the HST HUDF09 Data*, *Supplementary Information for Nature Letter*, doi: 10.1038/nature09717, (2011).
- [63] G.P. Smith, D.J. Sand, E. Egami, D. Stern and P.R. Eisenhardt, *Optical and Infrared Nondetection of the $z = 10$ Galaxy behind Abell 1835*, *Ap.J*, **636**, 575-581, (2006).
- [64] H. Arp, *A corrected velocity for the local standard of rest by fitting to the mean redshift of local group galaxies*, *A&A* **156**, No.1-2, 207-212, (1986).
- [65] W.G. Tifft, in *New Ideas in Astronomy*, eds. F. Bertola, J. Sulentic and B. Madore, (Cambridge Univ. Press), 173, (1988).
- [66] W.G. Tifft, Preprint of Steward Observatory No.1143, (1993). W.G. Tifft, *Redshift quantization - a review*, *Astrophysics and Space Science*, Vol.**227**, No.1-2/May, 25-39, (1995). W.G. Tifft, *Global redshift periodicities and variability*, *ApJ* **485**, Nu.2, 465-483, (1997).
- [67] L. Anderson, E. Aubourg, S. Bailey, et al., *The clustering of galaxies in the SDSS-III Baryon Oscillation Spectroscopic Survey: baryon acoustic oscillations in the Data Release 9 spectroscopic galaxy sample*, *Mon.Not.Roy.Astron.Soc.* **427**, Issue 4, 3435-3467, (2013), arXiv:1203.6594. C.C. Fulton and H.C. Arp, *The 2df redshift survey. I. Physical association and periodicity in quasar families*, *Ap.J*, **754**, 134, (10pp), (2012), doi:10.1088/0004-637X/754/2/134.
- [68] P.M. Hansen, *Astronomical redshifts of highly ionized regions*, *Astrophys Space Sci* **352**, 235244, (2014), doi:10.1007/s10509-014-1910-2.
- [69] O. Davis Johns, *Analytical Mechanics for Relativity and Quantum Mechanics*, pp.483-485, (Oxford Univ. Press), (2005).
- [70] D. Bohm, *Phys.Rev.* **85**, pp.166 and 180, (1952). D. Bohm, *Phys.Rev.* **87**, 389, (1952).
- [71] G. Burbidge and M. Burbidge, *Quasi-Stellar Objects*, (Freeman, San Francisco, 1967). H. Arp, E. Giraud, J.W. Sulentic and J.P. Vigier, *A&A* **121**, No.1, 1,26 (1983). H. Arp, *Quasars, redshifts and controversies*, (Interstellar Media, Berkeley), (1987). Zhu Xing-fen and Chu Yao-quan, *Periodic redshift distribution of quasars associated with low redshift galaxies*, *Chinese Astronomy and Astrophysics* Vol.**14**, Issue 4, 429-436, (December 1990). G. Burbidge and A. Hewitt, *Sky and*

- Telescope, **32**, (December 1994). Gong Shu-mo and Xia Chang-li, *Statistical analysis of emission and absorption lines of quasars. II. An analysis of 6761 quasars*^{1,*2}*, Chinese Astronomy and Astrophysics Vol.**23**, Issue 1, 17-21, (January-March 1999). H. Arp, *Arguments for a Hubble Constant near $H_0 = 55$* , Ap.J **571**, 615618, (2002). G. Burbidge, E.M. Burbidge and H. Arp, *The nature of the ultraluminous X-ray sources inside galaxies and their relation to local QSOs*, A&A **400**, L17-L19 (2003), astro-ph/0211139. E.M. Burbidge & G. Burbidge, *The Ejection of QSOs from AGN: A Phenomenon that Cannot be Denied*, in Suzy Collin, Franoise Combes and Isaac Shlosman, eds., Active Galactic Nuclei: from Central Engine to Host Galaxy, meeting held in Meudon, France, 23-27 July 2002, (ASP Conference Series, v. **290**, Astronomical Society of the Pacific, San Francisco), p.75, (2003). H. Arp, E.M. Burbidge, and G. Burbidge, *The double radio source 3C343.1: A galaxy-QSO pair with very different redshifts*, (January 2004), astro-ph/0401007v1. H. Arp, C.M. Gutierrez and M. Lopez-Corredoira, *New optical spectra and general discussion on the nature of ULX's*, A&A **418**, 877-883, (2004), astro-ph/0401103. D.G. Russell, *Intrinsic Redshifts and the TullyFisher Distance Scale*, Astrophysics and Space Science **299**, 4, 405-418, (2005). D.G. Russell, *Evidence for Intrinsic Redshifts in Normal Spiral Galaxies*, Astrophysics and Space Science 298:4, 577-602 (2005). P. Galianni, E.M. Burbidge, H. Arp, V. Junkkarinen, G. Burbidge and S. Zibetti, *The Discovery of a High-Redshift X-Ray – Emitting QSO Very Close to the Nucleus of NGC 7319*, Ap.J **620**, 88-94, (2005), astro-ph/0409215v1.
- [72] H. Arp, E.M. Burbidge, *X-ray Bright QSO's around NGC 3079*, (April 2005), astro-ph/0504237v1. H. Arp, *A Galaxy Cluster Near NGC 720*, (October 2005), astro-ph/0510173v1. E.M. Burbidge, G. Burbidge, H.C. Arp, and W.M. Napier, *An anomalous concentration of QSOs around NGC3079*, (October 2005), astro-ph/0510815v1. G. Burbidge, E.M. Burbidge, H.C. Arp, and W.M. Napier, *Ultraluminous x-ray sources, high redshift QSOs and active galaxies*, (May 2006), astro-ph/0605140v1. H. Arp, E.M. Burbidge and D. Carosati, *Quasars and Galaxy Clusters Paired Across NGC 4410*, (May 2006), astro-ph/0605453v1. H. Arp, D. Carosati, *A concentration of quasars around the jet galaxy NGC1097*, (May 2007), astro-ph/0706.0143v1. H. Arp, D. Carosati, *M31 and Local Group QSO's*, (June 2007), astro-ph/0706.3154v1. M.B. Bell, *Further Evidence That the Redshifts of AGN Galaxies May Contain Intrinsic Components*, Ap.J.Lett. **667**, L129-132, DOI: 10.1086/522337, (October 2007). H. Arp, *Quasars and the Hubble Relation*, (November 2007), astro-ph/0711.2607v1. H. Arp, *Dark Energy and the Hubble Constant*, (December 2007), astro-ph/0712.3180v1. H. Arp, C. Fulton, *A Cluster of High Redshift Quasars with Apparent Diameter 2.3*, (February 2008), astro-ph/0802.1587v1. H. Arp, C. Fulton, *The 2dF Redshift Survey II: UGC 8584 - Redshift Periodicity and Rings*, (March 2008), astro-ph/0803.2591. N.E. Strand, R.J. Brunner, A.D. Myers, *AGN Environments in the Sloan Digital Sky Survey. I. Dependence on Type, Redshift, and Luminosity*, ApJ **688**, 180, doi: 10.1086/592099, (2008). M. Lopez-Corredoira, *Pending problems in QSOs*, (November 2009), arXiv:0910.4297v2 [astro-ph.CO].
- [73] T.M. Brown, T. Lanz, A.V. Sweigart, M. Cracraft, I. Hubeny, and W.B. Landsman, *New Observational Evidence of Flash Mixing on the White Dwarf Cooling Curve*, (20 Jan 2012), arXiv:1201.4204v1 [astro-ph.SR].
- [74] I. Ciufolini, and J.A. Wheeler, "Gravitation and Inertia", 141-144, (Princeton Univ. Press, New Jersey), (1995).
- [75] Ch.W. Misner, K.S. Thorne, J.A. Wheeler, Gravitation, (W.H. Freeman and Company), (1973).